



## รายงานการวิจัยฉบับสมบูรณ์

โครงการ : อิทธิพลของโครงสร้างผลึกต่อความว่องไวในการทำปฏิกิริยาของตัวเร่ง  
โครงสร้างนาโน

**The Influence of Crystal Framework on the Reactivity of Nanostructured Catalysts.**

โดย พศ. ดร. ดวงกมล กลีสัน

พฤษภาคม 2554

สัญญาเลขที่ RMU5180032

# รายงานการวิจัยฉบับสมบูรณ์

โครงการ: อิทธิพลของโครงสร้างผลึกต่อความว่องไวในการทำปฏิกิริยาของตัวเร่ง  
โครงสร้างนาโน

**The Influence of Crystal Framework on the Reactivity of Nanostructured  
Catalysts.**

## ผู้วิจัย

ผศ. ดร. ดวงกมล กลีสัน

## สังกัด

สาขาวิชาเคมี คณะวิทยาศาสตร์  
สถาบันเทคโนโลยีพระจอมเกล้าเจ้าคุณทหารลาดกระบัง

## สนับสนุนโดย

สำนักงานกองทุนสนับสนุนการวิจัย และ สำนักงานคณะกรรมการการอุดมศึกษา

(ความเห็นในรายงานผลการวิจัยเป็นของผู้วิจัย สกอ. และ สาว. ไม่จำเป็นต้องเห็นด้วยเสมอไป)

## บทคัดย่อ

รหัสโครงการ: RMU5180032

ชื่อโครงการ: อิทธิพลของโครงสร้างผลึกต่อความว่องไวในการทำปฏิกิริยาของตัวเร่ง  
โครงสร้างนาโน

ชื่อนักวิจัยและสถาบัน: ผศ. ดร. ดวงกมล กลีสัน สาขาวิชาเคมี คณะวิทยาศาสตร์  
สถาบันเทคโนโลยีพระจอมเกล้าเจ้าคุณทหารลาดกระบัง

Email address: ktduangk@kmitl.ac.th

ระยะเวลาโครงการ: พฤษภาคม 2551 – พฤษภาคม 2554

งานวิจัยนี้ได้นำวิธีการคำนวณทางกลศาสตร์ค่อนต้ม มาใช้ในการวิเคราะห์กลไกปฏิกิริยาอย่างมีระบบในปฏิกิริยา skeletal isomerisation ของ cis-butene เป็น isobutene ในตัวเร่งซีโอໄล์ต์ชนิด ferrierite โดยกลไกปฏิกิริยาที่ศึกษามีสองชนิดได้แก่ ชนิดแรกเรียกว่า conventional mechanism ซึ่งกลไกปฏิกิริยาจะเกิดผ่าน alkoxide intermediate ที่เป็นโครงสร้างที่เสถียร ส่วนชนิดที่สองกลไกจะเกิดผ่าน carbenium ions

แบบจำลองที่ใช้ในการศึกษากลไกปฏิกิริยาข้างต้น ใช้แบบจำลองขนาด 27T cluster เพื่อแทนซีโอໄล์ต์ชนิด ferrierite ซึ่งใช้ระเบียบวิธีการคำนวณ density functional theory (M062X DFT functional)

ผลจากการคำนวณจาก พบร้าโครงสร้างที่เป็น carbenium ions จะมีความเสถียรน้อยกว่าโครงสร้างที่เป็น alkoxide intermediates ที่เกิดขึ้นในกลไกที่เป็นแบบ conventional mechanism โดยพิจารณาจากขั้นกำหนดอัตราที่มีพลังงานต่ำกว่าประมาณ 10 kcal/mol การที่พลังงานที่สูงกว่าอธิบายได้ว่ามีการเกิด intermediate ขึ้นภายในโพรงของซีโอໄล์ต์ ซึ่งจากข้อมูลที่มีอยู่สามารถสรุปได้ว่า จะเกิด intermediate ขึ้นมาในระหว่างการเกิดปฏิกิริยา skeletal isomerisation ของ butene ใน ferrierite จะเกิดผ่านกลไกที่เกิด carbenium เท่านั้น ซึ่งผลการศึกษานี้สอดคล้องกับผลการทดลองที่ alkoxide intermediate จะเป็น species ที่พบในการทดลอง

**Keywords :** Zeolite catalysis, carbenium, alkoxide, skeletal isomerisation, QM, DFT, FER

## Abstract

**Project code: RMU5180032**

**Project title: The Influence of Crystal Framework on the Reactivity of Nanostructured Catalysts.**

**Investigator: Asstn. Prof. Dr. Duangkamol Gleeson**

**Department of Chemistry, Faculty of Science,**

**King Mongkut's Institute of Technology Ladkrabang**

**Email address:** [ktduangk@kmitl.ac.th](mailto:ktduangk@kmitl.ac.th)

**Project period:** **May 2008 – May 2011**

In this study, quantum mechanical calculations have been performed to systematically analyse two different reaction mechanisms for the skeletal isomerisation of cis-butene to isobutene in ferrierite zeolite. One involves a conventional mechanism that proceeds via stable alkoxide intermediates and the other one which proceeds via carbenium ions only.

The calculations were performed using 27T quantum mechanical cluster model representations of ferrierite, which is described using the M062X density functional.

Although the carbenium ion structures formed over the pathway are inherently less stable than the alkoxide intermediates formed in the conventional mechanism, the rate determining step is predicted to be almost 10 kcal/mol lower in energy. The higher barrier for the latter process is due to the inherent stability of the intermediates formed within the pore. This appears to suggest that while these intermediates are formed over the course of a reaction, the skeletal isomerisation of butenes in ferrierite only occurs via a carbenium based mechanism. This proposal is consistent with experimental results that alkoxide intermediates are experimentally observed species.

**Keywords** — Zeolite catalysis, carbenium, alkoxide, skeletal isomerisation, QM, DFT, FER

## EXECUTIVE SUMMARY

Quantum chemical calculations of model zeolites can be used to analyse the mechanisms of catalysis by the consideration of the relative energies, geometries, and interactions of the substrate, transition state, intermediate and product with the catalytic active site. A considerable amount of scientific resource has been devoted to the research of zeolites as replacements for traditional media that are employed as catalysts in the transformation of hydrocarbons. In particular, quantum mechanical (QM) simulations have been extensively employed to study concepts in zeolite catalysis since it is possible to study the energetics and structures of catalytic reactions, offering a unique way to rationalise experimental results.

Here we propose a study of a ferrierite (FER) zeolite, which is of considerable interest to industry at present for a number of potential applications. We focus on the skeletal isomerisation of n-butene to isobutene in FER which experimentally is found to be more selective in the formation of the desired end product, isobutene, because of its reduced acidity and smaller interconnecting channels.

We propose an investigation into the mechanism of skeletal isomerisation of n-butene within the FER pore via (a) a conventional monomolecular mechanism and (b) a dimerisation mechanism recently proposed, to see which is energetically more favourable. Importantly, we also explore the nature of the computational model by employing clusters of 27T model and simulate using DFT methods. Single point calculations of the full model are subsequently carried out at M062X functional with the 6-311+G(2df,dp) basis set used for the 6T region and 6-31G\* for the remainder. Additionally, the key bond distances, angles, interaction distances and charges for the stationary points derived from each model are rigorously compared to assess the differences that result from the different simulation conditions. This will provide useful insight into the strength and weakness of the different models.

## กิตติกรรมประกาศ

โครงการวิจัยนี้ได้รับทุนอุดหนุนจากสำนักงานคณะกรรมการการอุดมศึกษา และ สำนักงานกองทุนสนับสนุนการวิจัย คณบุคคลวิจัยขอขอบคุณหน่วยงานดังกล่าวที่ให้การสนับสนุนทุนวิจัยตลอดโครงการวิจัยนี้ จนได้จัดเป็นรูปเล่มรายงานฉบับสมบูรณ์ของงานวิจัยนี้

## สารบัญ

เรื่อง	หน้า
บทคัดย่อ	ก
ABSTRACT	ข
EXECUTIVE SUMMARY	ค
กิตติกรรมประกาศ	ง
สารบัญ	จ
สารบัญตาราง	ฉ
สารบัญรูป	ช
<b>บทที่ 1 บทนำ</b>	<b>1</b>
1.1 ที่มาและความสำคัญของปัญหา	1
1.2 วัตถุประสงค์ของงานวิจัย	2
1.3 ขอบเขตของงานวิจัย	2
1.4 ประโยชน์ที่คาดว่าจะได้รับ	5
<b>บทที่ 2 การทบทวนเอกสารและงานวิจัยที่เกี่ยวข้อง</b>	<b>6</b>
<b>บทที่ 3 วิธีการดำเนินงานวิจัย</b>	<b>8</b>
3.1 ขั้นตอนการดำเนินงานวิจัย	8
3.2 เครื่องมือและอุปกรณ์ที่ใช้	10
<b>บทที่ 4 ผลการวิจัยและอภิปราย</b>	<b>11</b>
4.1 Alkoxide based mechanism	12
4.2 Carbenium based mechanism	19
<b>บทที่ 5 สรุปผลการทดลอง</b>	<b>23</b>
เอกสารอ้างอิง	25
ภาคผนวก      OUTPUT	29

## สารบัญตาราง

ตารางที่	ชื่อตาราง	หน้า
----------	-----------	------

1	The energies of the stationary points obtained in this study. All energies are relative to the isolated energies of the zeolite model and cis-butene in the gasphase. $\Delta H$ corresponds to the energy of optimized complexes using the default basis set (M062X with cis-butene and zeolite 6T described by 6-31G(d) and 21T atoms using 3-21G). ZPE corresponds to the zero point correction energy for the optimized stationary points at the default level of theory. $\Delta H$ SP corresponds to the single point energy of the optimized stationary point performed as follows: M062X with cis-butene and zeolite 6T described by 6-311+G(2df,dp) and 21T atoms using 6-31G(d). The $\Delta G$ (SP+ZPE) value corresponds to the $\Delta H$ SP plus the ZPE correction obtained using the default basis set calculation. All values are reported in Kcal/mol..	13
---	---	----

## สารบัญรูป

รูปที่	ชื่อรูป	หน้า
1	Illustration of the proposed 10T:46T ONIOM model with a physisorped n- butene molecule. Stick indicates the inner layer and line indicates outer layer. The aluminium atom is illustrated as CPK.	3
2	An illustration of the 27T model used in this study (illustrated using a stick representation). The 6T region surrounding the the T2 Al atom and acidic center are described using the 6-31G(d) basis set (O atoms coloured red and Si grey). To include the confinement effect of the zeolite, the two pores that bisect the main 10T ring are also included in the calculation at using the 3-21G basis set (stick representation with all atoms coloured green).	11
3	A graphical illustration of the energetic associated with the alkoxide (Scheme A, grey solid line) and carbenium (Scheme B, dashed black line) based mechanisms. The stationary points found on the two pathways are illustrated in Figure 4, Figure 5.	12
4	Minima obtained in this study. 6T region denoted using a stick representation and the 21T region using wireframe. Atoms in the foreground have been removed to aid visualisation. Carbon atoms are numbered 1 to 4 to facilitate interpretation. Only the key zeolite atoms are numbered in the top left panel. Key distances and angles are illustrated.	15
5	Transition states obtained in this study. See Figure 4 caption for additional details.	16
6	Plot of the zero point corrected single point energies against the Mulliken charge on the alkene. Transition states are denoted by squares (red), carbenium ions by triangles (blue) and other minima using circles (black).	18
7	The tertiary butyl carbenium ion obtained in this study (CARB3). The key O---HC interactions are displayed to show the significant stabilizing effect the extended zeolite framework has on this stationary point.	21

## บทที่ 1

### บทนำ

#### 1.1 ที่มาและความสำคัญของปัญหา

The potential of zeolites has been identified by the chemical and petrochemical industries as an affordable, efficient material to selectively crack, alkylate or oligomerise hydrocarbons . . Benefits are widespread, including the production of chemical precursors such as isobutene, key in the production of petrol additive MTBE and ETBE used to increase the octane rating of fuel, or ethyl-benzene, an intermediate used in the production of polystyrene .

A considerable amount of scientific resource has been devoted to the research of zeolites as replacements for traditional media employed as catalysts in the transformation hydrocarbons. In particular, quantum mechanical (QM) simulations have been extensively employed to study concepts in zeolite catalysis, since it is possible to study the energetics and structures of catalytic reactions, offering a unique way to rationalise experimental results.

Here we propose a study of a medium pore zeolite ZSM-5, which is of considerable interest to industry at present for a number of potential applications. We focus on the skeletal isomerisation of n-butene to isobutene in ZSM-5 which experimentally shows a greater conversion of n-butenes than another medium pore zeolite, ferrierite (FER). Interestingly, the latter is found to be more selective in the formation of the desired end product, iso-butene, because of its reduced acidity and smaller interconnecting channels<sup>10</sup>. ZSM-5's increased reactivity is believed to be a result of its greater acidity, larger pore size and less restricted diffusion characteristics, exacerbated with time on stream<sup>10</sup>. As this selectivity difference arises with time on stream, it is effectively beyond the limits of current simulations.

We propose an investigation into the mechanism of skeletal isomerisation of n-butene within the more reactive ZSM-5 pore via (a) a conventional monomolecular mechanism and (b) a dimerisation mechanism recently proposed , to see which is energetically more favourable. Importantly, we shall also explore the nature of the computational model by employing gas phase clusters of varying size tetrahedra (3T, 5T, 10T) and

simulate using DFT methods. More rigorous ONIOM 46T models will also be simulated with an inner core of varying size, (3T, 5T, 10T) treated using DFT, and the remaining 46T region treated via an MM potential. Single point calculations of the full 46T model will subsequently be carried out at DFT levels to obtain more reliable energetics. Additionally, the key bond distances, angles, interaction distances and charges for the stationary points derived from each model will be rigorously compared using principal components analysis (PCA) to quantitatively assess the differences that result from the different simulation conditions. This will provide useful insight into the strength and weakness of each of the different models.

## 1.2 วัตถุประสงค์ของงานวิจัย

1. To model the catalytic reactivity of zeolite catalysts.
2. To elucidate experimental phenomena of zeolite catalysed reactions such as reaction mechanisms, and spectroscopic data.
3. To study the reaction mechanism of the catalytic conversion of butene to isobutene.
4. To analyse the structures and properties of zeolite active sites in an attempt to improve our understanding of the physical basis for the catalytic effect of zeolites.

## 1.3 ขอบเขตของงานวิจัย

This research project will involve the prediction of the stationary points and transition state structures of zeolite catalysts using state-of-the-art computational chemistry methods. The goal of this study is to elucidate the physical basis for experimental phenomenon in zeolite catalysts by probing their structure using quantum chemical calculations.

Of the variety of computational methods available, we choose to employ the ONIOM method which has been successful in reproducing experimental results. This method has also been applied to ZSM-5 on a number of previous occasions making it an ideal method to apply here. The system to be studied is illustrated in Figure 1 with a bound isobutene molecule.

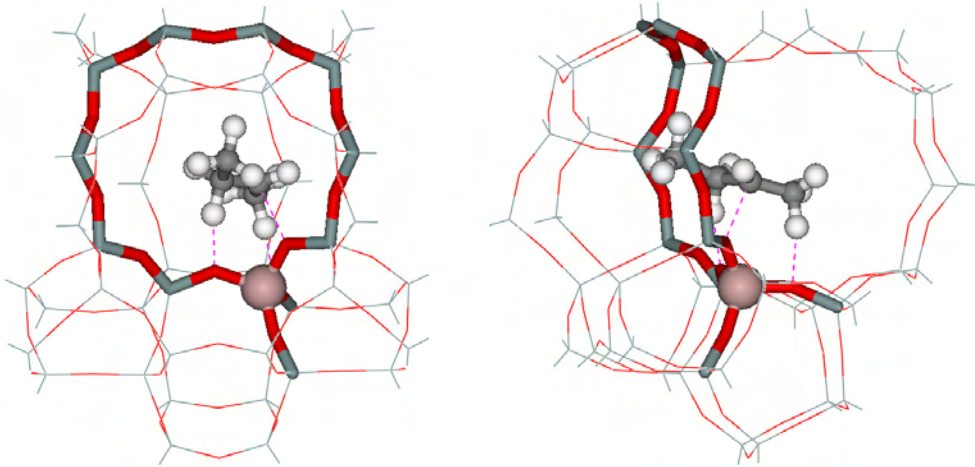


Figure 1. Illustration of the proposed 10T:46T ONIOM model with a physisorbed n-butene molecule. Stick indicates the inner layer and line indicates outer layer. The aluminium atom is illustrated as CPK.

The reactions to be studied are (a) the cis-trans isomerisation of butene and the skeletal isomerisation of 1-butene to isobutene via (b) a conventional, monomolecular mechanism and (b) an autocatalytic “dimerisation” mechanism. Calculations will initially focus on the cis-trans isomerisation to allow the most reliable computational system to be defined for the complex skeletal isomerisation studies.

ZSM-5, one of the most frequently studied zeolites in the theoretical literature, is to be represented in two distinct ways; (a) using small nT clusters and (b) using ONIOM nT:46T models. In each case three different QM cluster sizes (3T, 5T and 10T) will be used. The latter cluster sizes will also be employed as the inner QM region in the 46T ONIOM simulations. The models will be cut from the cross section of the straight channel and zigzag channel as used by others. The dangling bonds will be saturated with hydrogen atoms and these will be kept fixed during geometry optimization. Additionally, the 3T heavy atoms (Si, Al and O) and the substrate molecule will be allowed to relax for all 3T cluster and 3T:46T ONIOM calculations, while the 5T region and substrate molecule will be allowed to relax in the 5T, 5T:46T, 10T and 10T:46T

simulations. Based on the reports by Namuangruk et al. for propene oxide isomerisation in ZSM-576, this system should be sufficiently accurate to model the skeletal isomerisation reactions of butene.

All the calculations will be performed using the Gaussian 03 program . The 3T, 5T and 10T QM clusters will be optimized at the B3LYP/6-31G(d,p) level of theory with single points obtained using the optimized coordinates at the MP2/6-311++g(d,p) level. ONIOM simulations will employ the B3LYP/6-31G(d,p) level of theory for the inner region and the universal force field (UFF) for the outer region. All stationary points will be confirmed as such using frequency calculations. Single point energies will be obtained in two distinct ways; (a) at the MP2/6-311++g(d,p):UFF level on the optimized nT:46T system and (b) at the B3LYP/6-31G(d,p) level for the full 46T optimized system.

To extract as much information as possible from our QM calculations on 6 different alkenes, we will employ Principle Components Analysis (PCA) - , a widely used statistical technique in both zeolite simulation and cheminformatics - . PCA is a method for reducing the amount of data to be analyzed by exploiting the correlated nature of the variables within a dataset. Linear combinations of the correlated variables are taken such that the majority of the variance of the original data can be described by a smaller number of orthogonal components. The components can then be used to assess the similarities in the reaction structures and the nature of the structural differences in a quantitative fashion. This method will allow us to systematically assess the difference between the different cluster model structures and those from the ONIOM models. Finally, linear regression will be used to assess the relationship between the energetics and structure, as represented by key distances, angles, dihedrals and atomic Mulliken charges.

A summary of the key features and expected finding of this study are given below.

A. Cis/Trans Isomerisation

- Inter comparison of cluster and ONIOM models
- Analysis of stationary point properties using PCA
- Identification of the key differences between clusters and ONIOM
- Identification of the key differences between different sized clusters
- Relationship between energetic differences and structure

B. Butene Skeletal Isomerisation

- Comparison of the conventional and autocatalytic mechanisms
- Key differences between ONIOM DFT:UFF and DFT single point.
- Assessment of the agreement of theory with experimental results of de Menorval
- Relationship between energetic differences and structure

**1.4 ประโยชน์ที่คาดว่าจะได้รับ**

1. Improve our understanding of the catalytic conversion reactions of zeolites.
2. To increase our general understanding of zeolite action such that the design of selective zeolites for specific purposes may be realised.
3. To determine how well the current simulation methods are by trying to differentiate between experimental results.

The combination of modern computational hardware and quantum mechanical software can provide an alternative to experiment while also providing an insight into molecular mechanisms impossible to observe experimentally. In relation to zeolite chemistry, this not only allows us to interpret experiment but also potentially assess reactions not yet considered. These efforts will help to improve the properties of inorganic catalysts through the proposal of plausible reaction mechanisms from an accurate description of active site interactions. Knowledge of the reactions should help in the realisation of new, improved catalysts.

## บทที่ 2

### การทบทวนเอกสารและงานวิจัยที่เกี่ยวข้อง

Zeolites are important silicon based catalysts employed in the petrochemical industry to transform crude materials into refined products<sup>1,2</sup>. The desirable catalytic activity of these materials mainly arises due to; (a) the replacement of individual silicon atoms in the 3D lattice structure with aluminum, giving rise to a strong acidic center and/or (b) the presence of additional heavy metals in the zeolite pores<sup>3-5</sup>. Combined with the diverse range of three dimensional pore structures that such materials exhibit<sup>2,6-9</sup>, a range of useful chemical reactions can be catalyzed by these materials<sup>10,11</sup>. One application where such materials have proved particularly useful is in the catalytic cracking and skeletal isomerisation of hydrocarbons employed in the petrochemical industry<sup>2,10,12-14</sup>. The skeletal isomerisation of linear butenes to isobutene in FER has been extensively studied experimentally<sup>15-18</sup> given that the latter is an important chemical precursor<sup>19</sup>.

In this study the related catalytic conversion of cis-butene to iso-butene in the zeolite ferrierite (FER) is investigated. This zeolite is of significant interest from the point of view of butene isomerisation due to the high selectivity it displays for iso-butene compared to larger pore zeolites such as ZSM-5<sup>20,21</sup>. These differences arise due to the so called confinement effect of the unique zeolite lattice and their differing acidities<sup>6-8</sup>. There are still a number of uncertainties regarding the origin of the catalytic effect of zeolite on this reaction, including whether it occurs via a mono-molecular or pseudo bi-molecular route<sup>2</sup>.

Extensive experimentation has been undertaken on zeolites using techniques such as infra-red, UV, NMR and EPR spectroscopy<sup>22-24</sup>. In addition extensive use of theoretical methods have been reported in the literature. Quantum mechanical (QM) calculations of various types have been employed to elucidate aspects of zeolite catalysis including QM cluster calculations<sup>5,13,25</sup>, hybrid quantum mechanical/molecular mechanical (QM/MM)<sup>14,26</sup> and ONIOM methods<sup>27-29</sup>, as well as periodic DFT simulations<sup>30,31</sup>. In this study, a relatively large DFT cluster model of FER is employed to study the local effects of the pore structure on the skeletal isomerisation of cis-butene in the zeolite (Figure 2) since reports from Hansen et al suggest that such a sized cluster is needed to enable

the locations of high energy carbenium or carbonium ions<sup>32</sup>. The improved M062X DFT functional<sup>33-35</sup> is employed here as it has been used quite extensively to study aspects of zeolite catalysis recently<sup>7,13,28,35</sup>.

The investigations of Boronat et al<sup>36</sup> in the medium pore zeolite Theta-1 showed that the skeletal isomerisation reaction of linear butenes proceeds via two alkoxide intermediates (secondary and tertiary butyl) to the iso-butene product. The rate determining barrier is 22 kcal/mol and involve methyl group migration. No carbenium ion stationary points were reported in Theta-1 or in a related study on ZSM-5<sup>37</sup> by this author. Demuth et al investigated the related skeletal isomerisation of 2-pentene and they proposed that the most likely pathway involved the formation of high energy, but stable secondary carbenium ions as transient intermediates<sup>38</sup>. This differing result may be due to differences in the zeolite pore structures under investigation in the different studies since these are known to have a dramatic effect on the stability of carbenium ions<sup>39,40</sup>. Niemenan et al<sup>41</sup> has also assessed aspects of alkoxide species stabilities in FER using alkenes between 3 to 5 carbons in length. They showed that the stability of the alkoxy formed was very sensitive to the steric bulk of the alkene in question. In addition, a number of studies have discussed the importance of carbenium ions and their relevance in skeletal isomerisation of alkenes<sup>28,40,42-44</sup>. Tuma et al<sup>42,43</sup>, followed by Boronat et al<sup>40</sup>, concluded that carbenium ions should exist as true, albeit short lived reaction intermediates.

This study considers the skeletal isomerisation of linear butenes to iso-butene in FER the light of the most recent publications in the area. Both a conventional mechanism akin to that proposed by Boronat et al<sup>36,40</sup> that proceeds via alkoxide intermediates, and one that proceeds via carbenium based intermediates<sup>39</sup> is investigated. The zeolite FER has been chosen for this study due to its widespread use in skeletal isomerisation reactions<sup>15-18</sup> and (b) due to its rather small pore cavity which presumably makes carbenium ion formation more likely when compared to larger pore zeolites such as ZSM-5. The results are then contrasted with related theoretical studies which have been performed in either other zeolites and/or using similar alkenes: Theta-1<sup>40</sup>, ZSM-22<sup>36,38</sup>, ZSM-5<sup>37</sup> and FER<sup>28,41,42</sup> or generic zeolite models<sup>45</sup>.

## บทที่ 3

### วิธีการดำเนินงานวิจัย

#### 3.1 ขั้นตอนการดำเนินงานวิจัย

1. Build a number of structural models, i.e., clusters and zeolite frameworks.
2. Study the conversion of trans-butene to cis-butene in the gas phase and compare with the results from framework (active site's surrounding environment) of the zeolite.
3. Interpret the effect of the different active sites on the reaction and determine whether we can differentiate between the known experimental results using the ONIOM models.
4. Propose the mechanism for the reaction and interpret the results. Build a number of structural models, i.e., clusters and embedded clusters.
5. Build a number of structural models, i.e., clusters and zeolite frameworks.
6. Study the conversion of n-butene to isobutene in the framework (active site's surrounding environment) of the zeolite.
7. Study the reaction profile for the catalytic conversion of n-butene to isobutene.
8. Propose the mechanism for the reaction and interpret the results.
9. Build a number of structural models.
10. Study the autocatalytic conversion of n-butene to isobutene in the framework (active site's surrounding environment) of the zeolite.
11. Study the reaction profile for the autocatalytic conversion of n-butene to isobutene.
12. Propose the mechanism for the reaction and interpret the results
13. Compare the results from autocatalytic conversion calculations to those calculated based on the proposed mechanism in the second year.

Recent calculations on FER have used the cluster approach<sup>7</sup>, the ONIOM approach<sup>28</sup> and periodic methods<sup>42,46</sup> to good effect to elucidate aspects of its catalytic function. Due to the relative simplicity of the cluster approach, and the ability of relatively large clusters to describe high energy intermediates formed within zeolite systems<sup>32</sup>, the cluster method was chosen for this study. The cluster model of FER was generated using the X-ray diffraction data in Material Studio<sup>47</sup>. FER has a 2 dimensional pore structure with a large main 10T channel bisected by smaller 8T channels. A 27T cluster

model was carved from the X-ray coordinates, encompassing 2 complete pores either side of the 10T central ring. The bronsted acid site was created by replacing a silicon atom located at the T2 position of the 10T ring with an aluminium atom<sup>7,41</sup>. The 6T region of the cluster model surrounding the T2 site and acidic oxygen using the 6-31G(d) basis set and more distant atoms using the 3-21G basis set (Figure 2). This approach has been used in the past to allow a large QM cluster of a zeolite to be simulated in a reasonable amount of time<sup>48,49</sup>. The 3-21G basis set does appear to be sufficient to describe longer range effects based on the reports of Yumura et al<sup>49</sup>. This resulted in a model system with a total of 1226 basis functions.

The 6T region surrounding the T2 site and acidic oxygen was excised from the original X-ray coordinates with bonds cut across the O-Si bond. To avoid issues due to overly strong polarization due to the presence of OH groups, bonds were cut across the Si-O bonds for the more remaining 21T atoms<sup>46</sup>. This type of approach is similar to that employed to Zhao et al in their validation of the M062X functional for zeolite based applications<sup>35</sup>. To maintain the overall shape of the zeolite all terminal hydrogen atoms in the 6T region were fixed while only silicon atoms beyond this region were fixed. This allowed the electronegative oxygen atoms, which are directed into the FER pore, to subtly alter their positions over the course of the simulated reaction, thereby allowing better stabilization of the reactive species formed. Boronat et al note that the lack of flexibility in the zeolite lattice is one of the key issues in estimating the energies of intermediates in QM models of zeolites<sup>40</sup>.

All geometry optimizations were performed using M06-2X functional in Gaussian 03<sup>50</sup> modified to use the Minnesota Density Functionals Module 3.1 by Zhao and Truhlar<sup>33</sup>. Minima and transition states were fully characterized as stationary points in the complete 27T model, in all cases displaying zero and one single negative frequently, respectively. Zero point energy corrections to the energetic were therefore possible. Single point energies of optimized coordinates were subsequently obtained using the M062X functional with the 6-311+G(2df,dp) basis set used for the 6T region and 6-31G\* for the remainder.

With regards to model validity, the skeletal isomerization of linear butenes to isobutene has previously been studied by Boronat et al in Theta-1 using a 20T model of that zeolite<sup>36</sup>. The authors reported that the results were in agreement with periodic models that include longer range effects of the zeolite lattice<sup>36,40</sup>. This finding should mean that the results obtained here from a larger 27T model of FER are likely to be of reasonably accuracy.

### 3.2 เครื่องมือและอุปกรณ์ที่ใช้

1. High Performance Computer
2. Gaussian 98 Software
3. Statistical Analysis Software

## บทที่ 4

### ผลการทดลองและอภิปราย

The energetic results obtained from the calculations are reported in Table 1 and Figure 2. The structural parameters of the optimized geometries are displayed in Figure 3 for minima and Figure 4 for transition states. The energies of the optimized complexes are given in Table 1 along with their corresponding zero point correction and the single point energies. The single point and ZPE corrected energies are found to be in good agreement with the energies obtained at the original level of theory. All energies discussed henceforth correspond to the single point energies (M062X with 6-311+G(2df,dp) for cis-butene, and the 6T region and 6-31G(d) for 21T region) including zero point energy corrections, and are expressed relative to the isolated reagents unless otherwise stated.

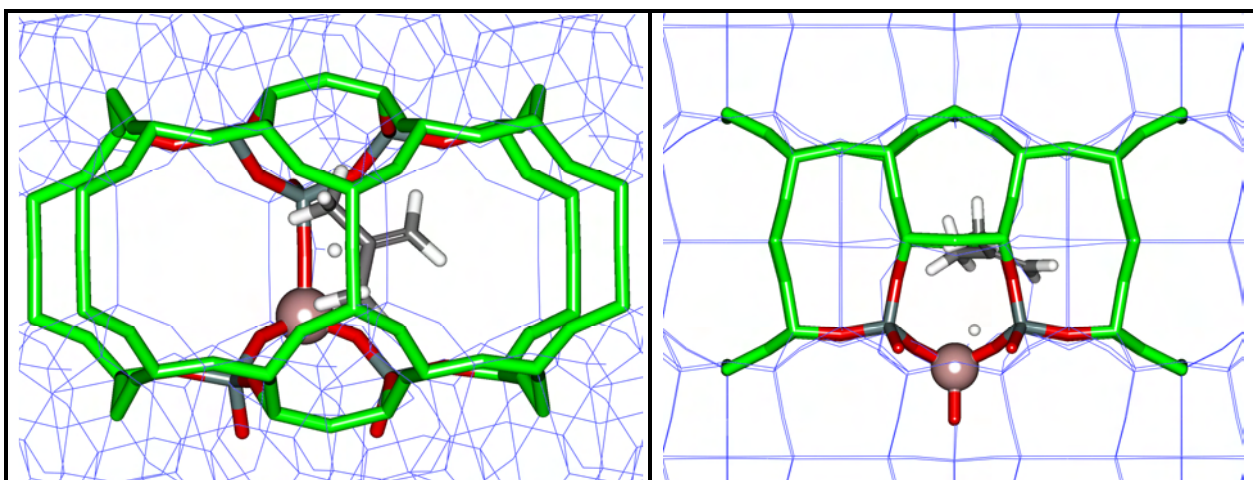


Figure 2 An illustration of the 27T model used in this study (illustrated using a stick representation). The 6T region surrounding the the T2 Al atom and acidic center are described using the 6-31G(d) basis set (O atoms coloured red and Si grey). To include the confinement effect of the zeolite, the two pores that bisect the main 10T ring are also included in the calculation at using the 3-21G basis set (stick representation with all atoms coloured green).

The skeletal isomerisation of cis-butene is first discussed in the context of the more conventional alkoxide based mechanism followed by a discussion on the relative likelihood of a carbenium based mechanism existing in this zeolite.

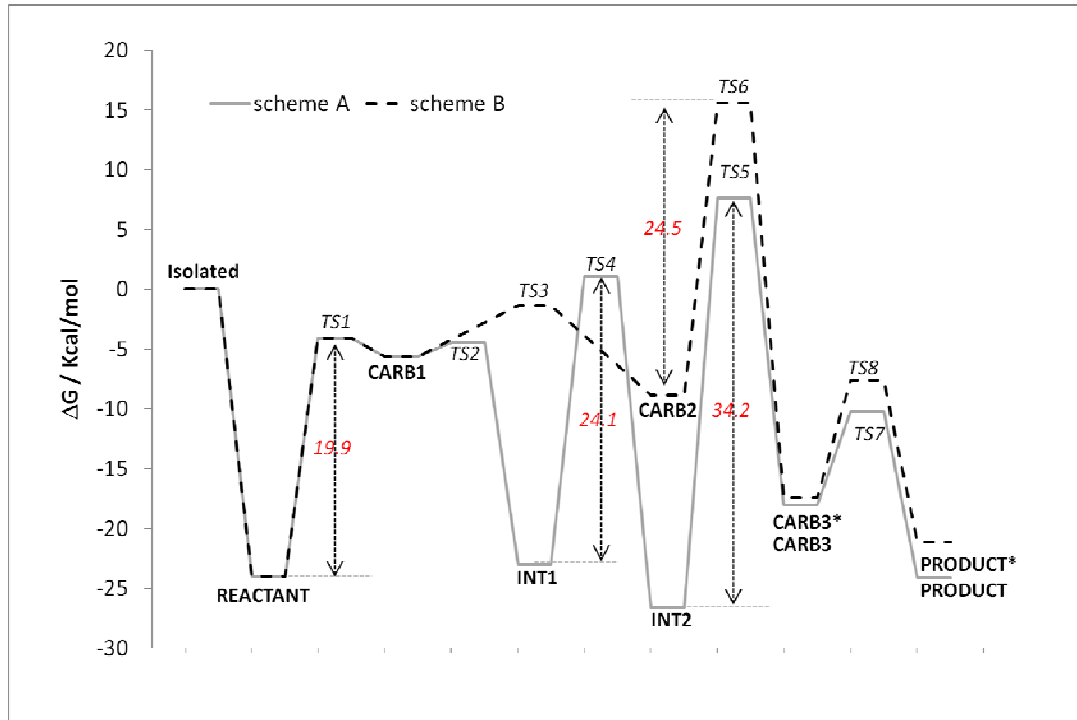


Figure 3 A graphical illustration of the energetic associated with the alkoxide (Scheme A, grey solid line) and carbenium (Scheme B, dashed black line) based mechanisms. The stationary points found on the two pathways are illustrated in Figure 4, Figure 5.

#### 4.1 Alkoxide based mechanism

The traditional uni-molecular mechanism of butene isomerisation begins with the formation of the adsorbed alkene-FER complex. The estimated adsorption energy of 1-butene is -18.9 kcal/mol in Theta-1<sup>51</sup> and -18.4 kcal/mol for iso-butene in FER<sup>42</sup>. Thus, the value of -23.8 kcal/mol obtained here for cis-butene adsorbed to FER appears reasonable especially given that it is less sterically hindered than iso-butene. The  $\pi$ -complex displays short C---H<sub>z</sub> interactions as expected (2.11 and 2.20 Å) while the C=C bond distance is only slightly elongated compared to the isolated gasphase value (1.34 vs 1.33 Å).

Table 1 The energies of the stationary points obtained in this study. All energies are relative to the isolated energies of the zeolite model and cis-butene in the gasphase.

$\Delta H$  corresponds to the energy of optimized complexes using the default basis set (M062X with cis-butene and zeolite 6T described by 6-31G(d) and 21T atoms using 3-21G). ZPE corresponds to the zero point correction energy for the optimized stationary points at the default level of theory.  $\Delta H$  SP corresponds to the single point energy of the optimized stationary point performed as follows: M062X with cis-butene and zeolite 6T described by 6-311+G(2df,dp) and 21T atoms using 6-31G(d). The  $\Delta G$  (SP+ZPE) value corresponds to the  $\Delta H$  SP plus the ZPE correction obtained using the default

basis set calculation. All values are reported in Kcal/mol.

Scheme-A	$\Delta H$	ZPE	$\Delta H$ SP	$\Delta G$ (SP+ZPE)
REACTANT	-22.82	-0.72	-23.25	-23.96
TS1	-4.51	0.44	-4.50	-4.06
CARB1	-6.91	0.42	-6.05	-5.63
TS2	-4.97	0.02	-4.45	-4.43
INT1	-21.65	-3.98	-19.03	-23.01
TS4	-1.31	-1.01	2.08	1.07
INT2	-29.80	-3.18	-23.41	-26.60
TS5	5.39	0.85	6.78	7.63
CARB3	-19.68	0.24	-18.29	-18.04
TS7	-11.38	1.42	-11.62	-10.21
PRODUCT	-20.34	-1.61	-22.50	-24.11
Scheme-B	$\Delta H$	ZPE	$\Delta H$ SP	$\Delta G$ (SP+ZPE)
REACT	-22.82	-0.72	-23.25	-23.96
TS1	-4.51	0.44	-4.50	-4.06
CARB1	-6.91	0.42	-6.05	-5.63
TS3	-1.46	-0.38	-0.94	-1.32
CARB2	-7.96	-0.36	-8.50	-8.87
TS6	13.36	2.11	13.48	15.59
CARB3 (C)	-19.16	0.68	-18.06	-17.38
TS8	-9.72	1.76	-9.38	-7.62
PRODUCT (C)	-18.62	-2.21	-18.94	-21.15

The skeletal isomerisation in Theta-1 begins with the formation of a secondary alkoxy complex in a concerted mechanism with simultaneous transfer of a proton from the zeolite to butene and the formation of a C-O bond<sup>36,40</sup>. The next step requires a methyl group shift, leading to the formation of a primary alkoxide intermediate. The carbon atom from which the methyl group migrates forms a C-O bond with an adjacent nucleophilic oxygen, while the migrating methyl satisfies the valence of the carbon atom whose C-O bond must break. The secondary alkoxide is found to be 6.9 kcal/mol higher in energy than the adsorbed complex compared to the primary alkoxide which is -2.9 kcal/mol lower. The rate determining step in theta one is the decomposition of the primary alkoxide to give adsorbed iso-butene. This final step requires the C-O bond of the primary alkoxide to break and the transfer of a proton to the zeolite which has a rate determining barrier of 32.7 kcal/mol. Iso-butene is found to be adsorbed to theta-1 only 0.7 kcal/mol higher in energy than 1-butene. Boronat et al note that these energies are likely to be upper limits given the 20T ring was not optimized (a 5T optimized model was inserted into the larger model and a single point energy calculated performed)<sup>36</sup>.

In FER, it is found that the formation of the initial alkoxide intermediate does not occur in a concerted manner, in contrast to than within the Theta-1 pore. Proton transfer from the O<sub>2</sub> atom of the zeolite to the C<sub>2</sub> of cis-butene via transition state one (TS1) leads to a stable carbenium ion 18.3 kcal/mol higher in energy than the adsorbed complex, with a barrier of 19.9 kcal/mol. The C<sub>2</sub>-C<sub>3</sub> distance of the adsorbed cis-butene increases to 1.45 Å in carbenium ion 1 (CARB1), intermediate between the double and single bond values expected for cis-butene in the gasphase (1.33 vs 1.50 Å respectively). TS1 is considerably closer in structure to the corresponding carbenium ion than adsorbed cis-butene as might be expected given the energetic differences. TS1 has a C<sub>2</sub>-C<sub>3</sub> distance that is very close to that of CARB1 (1.43 vs 1.45 Å), as well as the C<sub>2</sub>-H<sub>2</sub> distance of (1.14 vs 1.13 Å). The principal difference being the two is the C<sub>1</sub>-C<sub>2</sub>-C<sub>3</sub>-C<sub>4</sub> dihedral angle, which is 7° in CARB1 but 46.6° in TS1, facilitating the inductive stabilization of the positively charged carbon center in the former. CARB1 is stabilized by a single strong interaction formed between a C<sub>4</sub> hydrogen atom and the O<sub>3</sub> oxygen atom (1.98 Å), similar to those reported by Fang et al<sup>28</sup>.

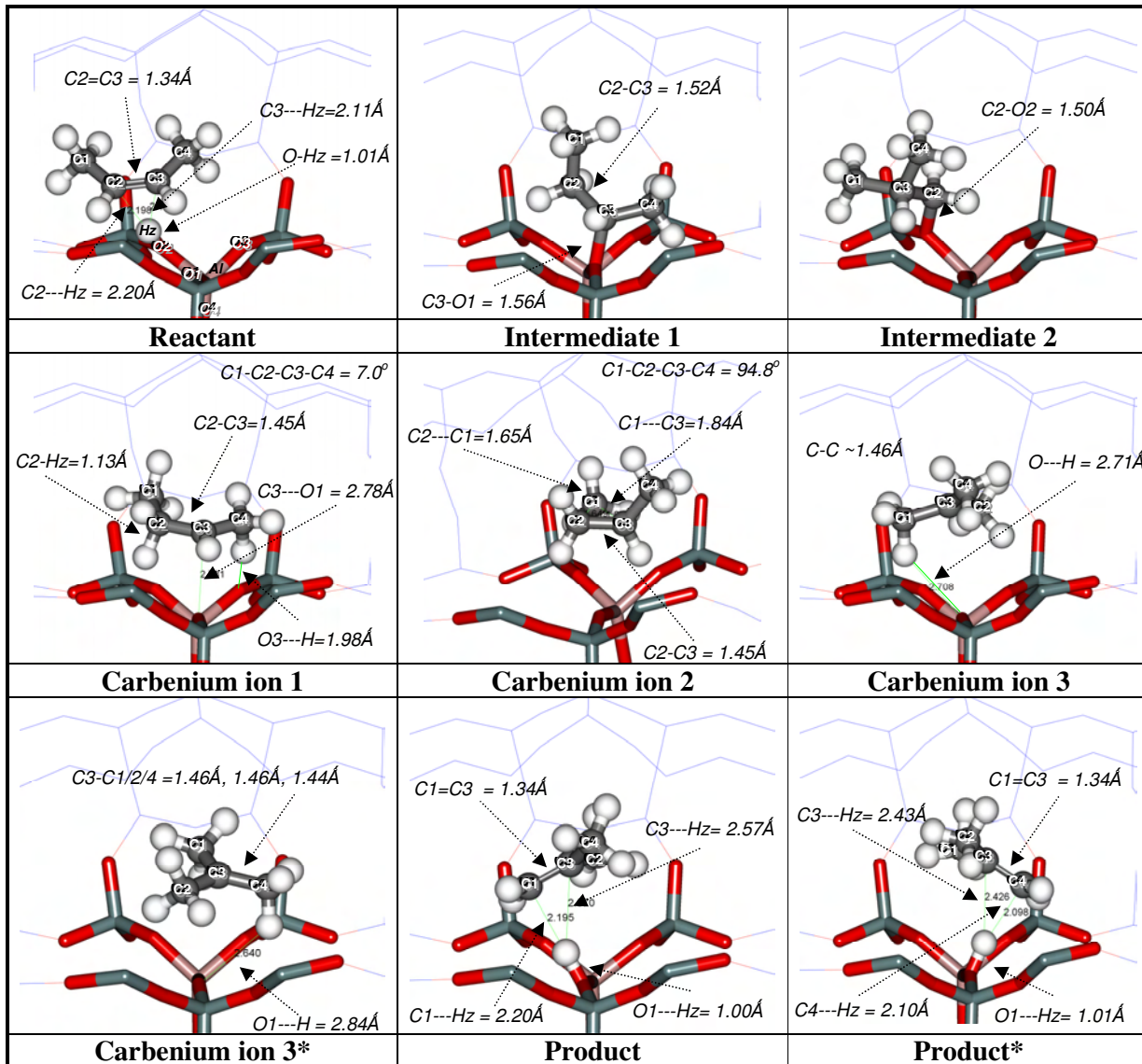


Figure 4 Minima obtained in this study. 6T region denoted using a stick representation and the 21T region using wireframe. Atoms in the foreground have been removed to aid visualisation. Carbon atoms are numbered 1 to 4 to facilitate interpretation. Only the key zeolite atoms are numbered in the top left panel. Key distances and angles are illustrated.

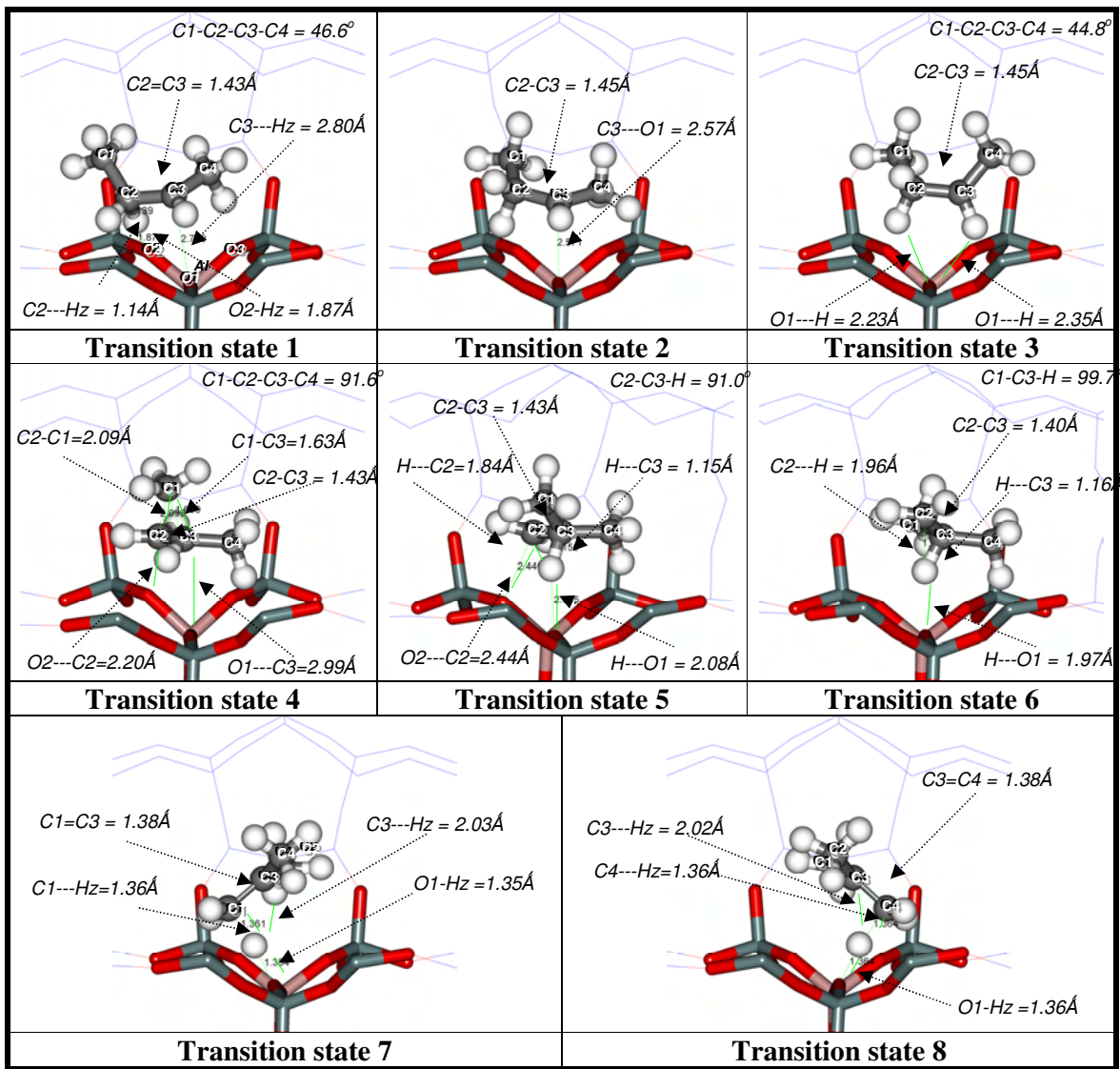


Figure 5 Transition states obtained in this study. See Figure 4 caption for additional details.

CARB1 can decompose in the forward direction to a secondary alkoxide intermediate by traversing a barrier of just 1.2 kcal/mol. The C3-O1 distance in TS2 is 2.57 Å, decreasing to 1.56 Å in the alkoxide intermediate (INT1). This structure is ~ 1kcal/mol lower in energy than the adsorbed cis-butene, lower than that reported by Boronat et al in Theta-1 (6.9 kcal/mol). This difference is not surprising given that the same authors show that alkoxides formed in Mordenite were shown to be heavily dependent on the T position<sup>39</sup>, as do others<sup>41</sup>.

Intermediate 2 (INT2) is formed when the methyl group (C1) migrates from C2 to C3. This requires the O1-C3 bond to break and the O1-C3 bond to form in the process. The transition state (TS4) displays a partial C2=C3 double bond as observed by the 1.43 Å distance. This facilitates the migration of the methyl group between these two atoms. The C1-C2 distance is 2.09 Å and the C3-C1 distance is 1.63 Å while the C2-O2 and O1-C3 distances are 2.20 Å and 2.99 Å respectively. The barrier of 24 kcal/mol is consistent with that observed by Boronat et al in Theta-1 (25.8 kcal/mol). The secondary alkoxide is 2 kcal/mol higher in energy than the adsorbed isobutene in FER from the work of Tuma et al<sup>42</sup>, which is consistent with what is found here (2.5 kcal/mol).

TS5 separates INT2 from carbenium ion 3, and not the product as is found in Theta-1. The breaking of the O2-C2 bond sees the migration of the hydrogen atom attached to C3 to C2 as the double bond begins to form. Proton transfer from this tertiary center to the zeolite was not observed due to the instability of the primary carbenium center that forms at C2. TS5 therefore displays a C2-O2 distance of 2.44 Å. The C3-H distance is 1.15 Å the C2-C3 distance is 1.42 Å. Crucially, the C2-C3-H angle is 91.0° indicating that the proton is in the process of migrating across the C2-C3 bond. This finding is consistent that the stability of carbenium ions are dependent on the accessibility of the acidic oxygen positions<sup>28,39</sup>. This barrier is 34.2, comparable to the final rate determining step found by Boronat et al in Theta-1 (32.7 kcal/mol)<sup>36</sup>.

The tertiary butyl carbenium ion (CARB3) displays C-C distances of approximately 1.46 Å. Due to the unique pore dimensions, the tertiary butyl carbenium ion can make significant interactions with the zeolite. In fact, all 9 hydrogen atoms are found to make significant interactions with the zeolite. The 9 shortest C-H---O interactions observed (one per alkyl H) were 4\*2.3 Å, 2.4 Å, 2.6 Å, 2\*2.7 Å and 2.9 Å (Figure 7), which would

explain the very low net change on the molecule compared to CARB1 (Figure 6). This observation is discussed in more detail in the following section.

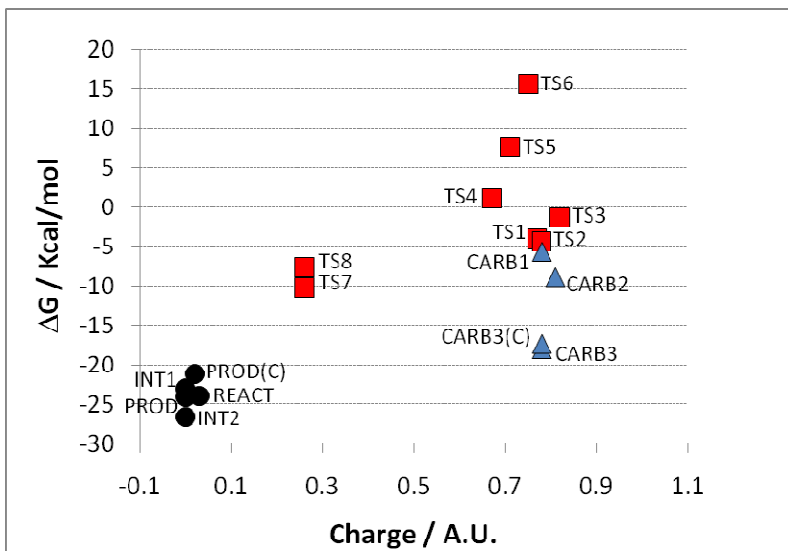


Figure 6 Plot of the zero point corrected single point energies against the Mulliken charge on the alkene. Transition states are denoted by squares (red), carbenium ions by triangles (blue) and other minima using circles (black).

CARB3 is found to be 6 kcal/mol higher in energy than the adsorbed cis-butene and iso-butene molecules. The latter energy is lower than the value reported very recently by Tuma et al (14 kcal/mol for tertiary butyl carbenium – adsorbed isobutene)<sup>42</sup>, but it is closer to their earlier reported value of 8.5 kcal mol<sup>43</sup>. Fang et al also report that the tertiary butyl carbenium ion is 14.7 kcal/mol higher in energy compared to adsorbed iso-butene molecules in ZSM5. However, in this case the larger 12T pore of ZSM5 is unlikely to provide the same level of stabilization to the carbenium ion of the smaller FER pore as discussed above.

Transition state 7 (TS7) connects CARB3 with the adsorbed iso-butene molecule. The C1-Hz distance in TS7 is 1.36 Å, the O2-Hz distance is found to be 1.35 Å and the C1-C3 distance is 1.38 Å. The barrier to reaction is considerably higher than that observed for CARB1 due to the inherent stability of the structure. The stabilization provided by the zeolite leads to a forward barrier to reaction of 8.2 kcal/mol (11.4 kcal/mol in the reverse direction). This value is somewhat higher than in the similar study of tert-butyl

carbenium ions in FER (3.3 kcal/mol) reported by Tuma et al<sup>42</sup> but might be a reflection of the different models and methodologies used.

The adsorbed iso-butene molecule is of equivalent energy to the adsorbed cis-butene molecule in line with that found in Theta-1<sup>51</sup>. Unlike the adsorbed cis-butene molecule, the interaction between the acidic site and the alkene double of iso-butene molecule is not approximately symmetric. In the latter case, the C1---Hz distance is found to be 2.20 Å and the C3---Hz distance 2.57 Å. However the symmetric nature of the iso-butene molecule, and the location of the O1 acidic atom at a less restricted part of the pore mean that the somewhat poorer interaction of iso-butene is somewhat compensated for by reduced steric repulsion.

#### 4.2 Carbenium based mechanism

The skeletal isomerism of cis-butene to iso-butene can proceed in a manner somewhat similar to that reported to Boronat et al in Theta-1. The key difference is that the very first, and very final steps, which are reported to be concerted in Theta-1, are found to be stepwise in FER, involving 2 stable carbenium ions. Nevertheless, the reported rate determining barrier for the alkoxide based mechanism found in FER is 34.2 kcal/mol, very close to that reported for Theta-1 at 32.7 kcal/mol.

The observation here that the skeletal isomerisation of linear butenes in FER will proceed in a concerted fashion, via carbenium ion intermediates, is perhaps not surprising given the recent work by Tuma et al on iso-butene carbenium ions in FER<sup>42</sup>. It has not however been reported if the skeletal isomerisation of linear butenes in FER can occur via a purely carbenium ion based process or at least now energetically favourable or not such a mechanism would be in comparison to one that proceeds via stable alkoxide intermediates. This is now discussed.

CARB1, formed by the transfer of the acidic proton to the C2 atom of cis-butene, can also react to form an additional carbenium ion, termed CARB2 here. For CARB2 to form, the C1-C2-C3-C4 dihedral angle must rotate from 7.0° in CARB1, to 44.8° in the transition state (TS3), before reaching a minima at 94.8° in CARB2. The barrier to this process is 4.3 kcal/mol. The minimum energy structure formed has a corresponding angle of 94.8°, and is 3.2 kcal/mol lower than CARB1 and 18.3 kcal/mol higher in

energy than the adsorbed iso-butene molecule. In this structure the methyl group lies intermediate between the C2 and C3 atoms and is akin to TS4 discussed before. The key difference between the two structures is that CARB2 makes two strong interactions between the migrating methyl group and the Al polarized O2 and O3 atoms. The interactions of 2.28 and 2.09 Å are observed indicating the interaction is particularly strong.

CARB2 can decompose to form CARB3\* (related to CARB3 in terms of their symmetry perpendicular to the 001 axis in FER) by completing the migration of the C1 methyl to the C3 position and the simultaneous migration of the C3 hydrogen atom across the C2=C3 bond as it increases in strength. In TS6 the methyl group has completely migrated. The C3-H distance is 1.16 Å, the C2-C3-H angle is 99.7°, and the C2=C3 distance is 1.40 Å. TS6 is found to be higher in energy than the related TS5 due to the fact that in the latter structure the breaking C2-O2 bond (coming from INT2) helps stabilize the structure, as can be seen by the considerably larger net Mulliken charge on the alkene (0.71 vs 0.75 respectively, Figure 6).

CARB3\* is slightly higher in energy than CARB3 (-17.4 vs -18.0 kcal/mol). This can be rationalized based on its slightly reduced interaction with the zeolite lattice, as can be seen from the marginally higher net Mulliken charge on the two alkenes (0.75 vs 0.71 respectively). CARB3\* reacts via TS8 to form the adsorbed iso-butene complex in a similar fashion to CARB3. The barrier is found to be 10.2 kcal/mol, 2.5 kcal/mol higher than TS7 which is associated with the CARB3. Again the less effective stabilization provided by the zeolite lattice explains the marginally higher barrier between these two related barriers (Figure 6). The adsorbed iso-butene molecule from this step is ~3 kcal/mol less well adsorbed than that arising from the alkoxide based mechanism (product\*). These subtle differences are in line with the accessibility of atoms reported by other researchers<sup>28,40,41,51</sup>.

The predicted rate determining energy barrier for the carbenium ion mediated process is 24.5 kcal/mol in FER, considerably lower than the 34.2 kcal/mol value obtained for the alkoxide based pathway. In fact, the key reason for the high energy barrier in the latter process is the inherent stability of alkoxide intermediates in acidic zeolites which explains why they are experimentally observed. In FER, the reverse barrier going from

INT2 to INT1 is just 27.7 kcal/mol, lower than the final rate determining step in the alkozide mediated process (34.2 kcal/mol), suggesting that the formation of iso-butene could still occur via a carbennium based route even though INT2 is highly likely to form given its low energy.

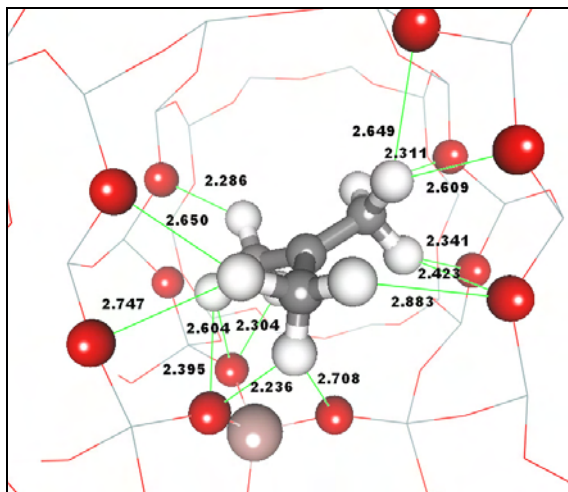


Figure 7 The tertiary butyl carbenium ion obtained in this study (CARB3). The key O---HC interactions are displayed to show the significant stabilizing effect the extended zeolite framework has on this stationary point.

Finally, the relationship between the relative energy of the stationary points obtained here and the net Mulliken charge observed on the alkene/alkane molecule is discussed. Fang et al reported that the stability of carbenium ions is proportional to the proton affinity or pKa of the molecule in question. In line with these finding, here it is found that the transition states that can most effectively delocalize the positive charge on proton transfer are generally of lower energy. TS7 and TS8 are not directly bonded to the proton explaining why the overall mulliken charge on this system is low. TS1, TS2 and TS3 are clustered together in terms of their energies and net Mulliken charges since they all contain secondary carbenium ion centers which are closely related to CARB1. TS4, TS5 and TS6 are related to INT1, INT2 and CARB2 respectively and their stability is correlated to their ability to delocalize their significant net positive charge. TS5 and TS6 both contain primary carbenium ion centers, but the latter interacts more favourably with the acidic center explaining its lower net charge and energy (see previous discussion). TS4 contains a ~secondary/tertiary carbenium center which has

two short C---O interactions with the acidic center explaining its lower positive charge than the other fully protonated transition states and even the carbenium stationary points.

This general trend between the ability to delocalize net positive charge and the relative energy does not hold for the carbenium ions. The energy is primarily dictated by whether the carbenium ion is located on a primary, secondary or tertiary center. Also important are the presence of rather stronger interactions with the oxygen atoms of the zeolite lattice which can lower the overall energy, even if this is not reflected in the Mulliken charges (Figure 7). CARB3 and CARB3\* are the lowest in energy since they are tertiary carbenium centers, followed by the secondary carbenium ions CARB2 and CARB1. As discussed earlier, CARB2 is lower in energy than CARB1 due to the more effective interactions it can make with the zeolite lattice oxygen atoms (even though its net Mulliken charge is higher).

These results confirm the findings of others that the accessibility of zeolite is very important for determining the stability of intermediates and carbenium ions formed with their pores. These results also suggest that QM models that employ relatively small flexible regions around the acidic center but fixed extended zeolite frameworks may miss a considerable amount of stabilization provided by oxygen atoms in the surrounding pore. These oxygen atoms here were found to move up to 0.3 Å in some cases over the course of the reaction pathways simulated.

## บทที่ 5

### สรุปผลการทดลอง

In this study the results from a systematic analysis of two different mechanisms for the skeletal isomerisation of cis-butene to iso-butene have been presented. One involves a conventional mechanism that proceeds via stable alkoxide intermediates and the other is one which proceeds via carbenium ions only.

A 27T cluster model has been used here for this purpose using the M062X DFT functional. Atoms in the 6T region have been treated using the 6-31G(d) basis set and those in the remainder of the cluster treated using the 3-21G basis set. All stationary structures have been confirmed as minima or transition states using the full model and basis set used for optimization. More accurate energies were obtained by taking single point energies (M062X with the 6T region treated using 6-311+G(2df,dp) and the remainder using 6-31G(d)) of the optimized coordinates and correcting for zero point energy effects.

The results obtained here are in good agreement with related reports in the literature where comparison are possible, giving confidence in the models used. The traditional concerted alkoxide based mechanism reported by Boronat et al<sup>36</sup> is not found in FER. In this study the mechanism is found to proceeds in a stepwise manner with proton transfer and nucleophilic attack occurring in separate steps, consistent with recent proposals by Tuma et al<sup>42</sup>. The rate determining step for this mechanism is found to be very close (~34 kcal/mol) to that reported by Boronat et al.

A purely carbenium based mechanism was also investigated, which did not require the formation of any alkoxide intermediates. Although the carbenium ion structures formed over the pathway are inherently less stable than the alkoxide intermediates formed in the more conventional mechanism, the rate determining step is predicted to be almost 10 kcal/mol lower in energy. The higher barrier for the conventional process is due to the inherent stability of the intermediates formed within the FER pore. This could suggest that while these intermediates are formed over the course of a reaction, the skeletal isomerisation of butenes in FER only occurs via the carbenium based mechanism. This proposal is consistent with experimental results that alkoxide intermediates are experimentally observed species.

With regards to the skeletal isomerisation of linear butene in larger zeolites such as ZSM-5, Rosenbach et al report that the tertiary butyl carbenium ion is 14 kcal/mol higher in energy than the adsorbed iso-butyl zeolite complex<sup>44</sup>. This is ~8 kcal/mol higher in energy than that observed here but it might suggest that a carbenium based mechanism in ZSM-5 might be close to isoenergetic with the more conventional alkoxide based mechanism. This proposal is currently under investigation.

## ເອກສາຣອ້າງອີງ

- (1) Choudary, N.; Newalkar, B. *Journal of Porous Materials* 2010, 1.
- (2) Kangas, M.; Kumar, N.; Harlin, E.; Salmi, T.; Murzin, D. Y. *Industrial & Engineering Chemistry Research* 2008, 47, 5402.
- (3) Brändle, M.; Sauer, J. *Journal of the American Chemical Society* 1998, 120, 1556.
- (4) Macht, J.; Carr, R. T.; Iglesia, E. *Journal of the American Chemical Society* 2009, 131, 6554.
- (5) Katada, N.; Suzuki, K.; Noda, T.; Sastre, G.; Niwa, M. *Journal of Physical Chemistry C* 2009, 113, 19208.
- (6) Lesthaeghe, D.; Van Speybroeck, V.; Waroquier, M. *Physical Chemistry Chemical Physics* 2009, 11, 5222.
- (7) Boekfa, B.; Pantu, P.; Probst, M.; Limtrakul, J. *Journal of Physical Chemistry C* 2010, 114, 15061.
- (8) Borgoo, A.; Tozer, D. J.; Geerlings, P.; De Proft, F. *Physical Chemistry Chemical Physics* 2009, 11, 2862.
- (9) Boronat, M.; Concepcion, P.; Corma, A.; Navarro, M. T.; Renz, M.; Valencia, S. *Physical Chemistry Chemical Physics* 2009, 11, 2876.
- (10) Corma, A. *Chemical Reviews* 1995, 95, 559.
- (11) Perego, C.; Ingallina, P. *Catalysis Today* 2002, 73, 3.
- (12) Vahteristo, K.; Sahala, K. M.; Laari, A.; Solonen, A.; Haario, H. *Chemical Engineering Science* 2010, 65, 4640.
- (13) Maihom, T.; Pantu, P.; Tachakritikul, C.; Probst, M.; Limtrakul, J. *Journal of Physical Chemistry C* 2010, 114, 7850.
- (14) Sun, Y. X.; Yang, J.; Zhao, L. F.; Dai, J. X.; Sun, H. *Journal of Physical Chemistry C* 2010, 114, 5975.
- (15) de Menorval, B.; Ayrault, P.; Gnepp, N. S.; Guisnet, M. *Journal of Catalysis* 2005, 230, 38.
- (16) Asensi, M. A.; Martínez, A. *Applied Catalysis A: General* 1999, 183, 155.
- (17) Guisnet, M.; Andy, P.; Gnepp, N. S.; Travers, C.; Benazzi, E. *Journal of the Chemical Society, Chemical Communications* 1995, 1685.
- (18) de Ménorval, B.; Ayrault, P.; Gnepp, N. S.; Guisnet, M. *Applied Catalysis A: General* 2006, 304, 1.

(19) van Donk, S.; Bus, E.; Broersma, A.; Bitter, J. H.; de Jong, K. R. *Journal of Catalysis* 2002, 212, 86.

(20) Yoon, J. W.; Lee, J. H.; Chang, J. S.; Choo, D. H.; Lee, S. J.; Jhung, S. H. *Catalysis Communications* 2007, 8, 967.

(21) Rutenbeck, D.; Papp, H.; Ernst, H.; Schwieger, W. *Applied Catalysis A: General* 2001, 208, 153.

(22) Hunger, M. *Microporous and Mesoporous Materials* 2005, 82, 241.

(23) Aerts, A.; Kirschhock, C. E. A.; Martens, J. A. *Chemical Society Reviews* 2010, 39, 4626.

(24) O'Neil Parker Jr, W. *Comments Inorg Chem* 2000, 22.

(25) Fellah, M. F.; Pidko, E. A.; van Santen, R. A.; Onal, I. *The Journal of Physical Chemistry C* 2011, 115, 9668.

(26) Zimmerman, P. M.; Head-Gordon, M.; Bell, A. T. *Journal of Chemical Theory and Computation* 2011, 7, 1695.

(27) Agarwal, V.; Conner, W. C.; Auerbach, S. M. *Journal of Physical Chemistry C* 2011, 115, 188.

(28) Fang, H. J.; Zheng, A. M.; Xu, J.; Li, S. H.; Chu, Y. Y.; Chen, L.; Deng, F. *Journal of Physical Chemistry C* 2011, 115, 7429.

(29) Ananikov, V. P.; Musaev, D. G.; Morokuma, K. *Journal of Molecular Catalysis A: Chemical* 2010, 324, 104.

(30) De Moor, B. A.; Ghysels, A.; Reyniers, M. F.; Van Speybroeck, V.; Waroquier, M.; Marin, G. B. *Journal of Chemical Theory and Computation* 2011, 7, 1090.

(31) Hansen, N.; Kerber, T.; Sauer, J.; Bell, A. T.; Keil, F. J. *Journal of the American Chemical Society* 2010, 132, 11525.

(32) Hansen, N.; Brüggemann, T.; Bell, A. T.; Keil, F. J. *The Journal of Physical Chemistry C* 2008, 112, 15402.

(33) Zhao, Y.; Truhlar, D. G. *Theoretical Chemistry Accounts* 2008, 120, 215.

(34) Hohenstein, E. G.; Chill, S. T.; Sherrill, C. D. *Journal of Chemical Theory and Computation* 2008, 4, 1996.

(35) Zhao, Y.; Truhlar, D. G. *Journal of Physical Chemistry C* 2008, 112, 6860.

(36) Boronat, M.; Viruela, P.; Corma, A. *Physical Chemistry Chemical Physics* 2001, 3, 3235.

(37) Gleeson, D. *Journal of Computer-Aided Molecular Design* 2008, 22, 579.

(38) Demuth, T.; Rozanska, X.; Benco, L.; Hafner, J.; van Santen, R. A.; Toulhoat, H. *Journal of Catalysis* 2003, 214, 68.

(39) Boronat, M.; Viruela, P. M.; Corma, A. *J Am Chem Soc* 2004, 126, 3300.

(40) Boronat, M.; Corma, A. *Applied Catalysis A: General* 2008, 336, 2.

(41) Nieminen, V.; Sierka, M.; Murzin, D. Y.; Sauer, J. *Journal of Catalysis* 2005, 231, 393.

(42) Tuma, C.; Kerber, T.; Sauer, J. *Angew Chem Int Ed Engl* 2010, 49, 4678.

(43) Tuma, C.; Sauer, J. *Angew Chem Int Ed Engl* 2005, 44, 4769.

(44) Rosenbach, N.; dos Santos, A. P. A.; Franco, M.; Mota, C. J. A. *Chemical Physics Letters* 2010, 485, 124.

(45) Svelle, S.; Kolboe, S.; Swang, O. *The Journal of Physical Chemistry B* 2004, 108, 2953.

(46) Mazar, M. N.; Al-Hashimi, S.; Bhan, A.; Cococcioni, M. *Journal of Physical Chemistry C* 2011, 115, 10087.

(47) Material Studio 4.0; Accelrys

(48) Yang, G.; Zhou, L.; Liu, X.; Han, X.; Bao, X. *Chemistry* 2011.

(49) Yumura, T.; Takeuchi, M.; Kobayashi, H.; Kuroda, Y. *Inorganic Chemistry* 2008, 48, 508.

(50) Frisch, M. J.; Trucks, G. W.; Schlegel, H. B.; Scuseria, G. E.; Robb, M. A.; Cheeseman, J. R.; Montgomery, J., J. A.; Vreven, T.; Kudin, K. N.; Burant, J. C.; Millam, J. M.; Iyengar, S. S.; Tomasi, J.; Barone, V.; Mennucci, B.; Cossi, M.; Scalmani, G.; Rega, N.; Petersson, G. A.; Nakatsuji, H.; Hada, M.; Ehara, M.; Toyota, K.; Fukuda, R.; Hasegawa, J.; Ishida, M.; Nakajima, T.; Honda, Y.; Kitao, O.; Nakai, H.; Klene, M.; Li, X.; Knox, J. E.; Hratchian, H. P.; Cross, J. B.; Bakken, V.; Adamo, C.; Jaramillo, J.; Gomperts, R.; Stratmann, R. E.; Yazyev, O.; Austin, A. J.; Cammi, R.; Pomelli, C.; Ochterski, J. W.; Ayala, P. Y.; Morokuma, K.; Voth, G. A.; Salvador, P.; Dannenberg, J.; Zakrzewski, V. G.; Dapprich, S.; Daniels, A. D.; Strain, M. C.; Farkas, O.; Malick, D. K.; Rabuck, A. D.; Raghavachari, K.; Foresman, J. B.; Ortiz, J. V.; Cui, Q.; Baboul, A. G.; Clifford, S.; Cioslowski, J.; Stefanov, B. B.; Liu, G.; Liashenko, A.; Piskorz, P.; Komaromi, I.; Martin, R. L.; Fox, D. J.; Keith, T.; Al-Laham, M. A.; Peng, C. Y.; Nanayakkara, A.; Challacombe, M.; Gill, P. M. W.; Johnson, B.; Chen, W.; Wong, M. W.; Gonzalez, C.; Pople, J. A. Gaussian 03, Revision C.02; Gaussian, inc: Wallingford CT, 2004.

(51) Boronat, M.; Zicovich-Wilson, C. M.; Viruela, P.; Corma, A. *The Journal of Physical Chemistry B* 2001, 105, 11169.

## ภาคผนวก

**OUTPUT** จากโครงการวิจัยที่ได้รับทุนจาก สกอ.

### ผลงานตีพิมพ์ในวารสารวิชาการนานาชาติ

1. Gleeson, D. Skeletal Isomerization of butene in Ferrierite. Assessing the energetic and structural differences between carbenium and alkoxide based pathways. *J. Phys. Chem. C*, 2011, Submitted.
2. Gleeson, D. A theoretical study of cis-trans isomerisation in H-ZSM5: probing the impact of cluster size and zeolite framework on energetic and structure, *J. Comput. Aided Mol. Des.*, 2008, 22(8): 579-85.

**Skeletal Isomerization of butene in Ferrierite. Assessing the energetic and structural differences between carbenium and alkoxide based pathways.**

Journal:	<i>The Journal of Physical Chemistry</i>
Manuscript ID:	Draft
Manuscript Type:	Article
Date Submitted by the Author:	n/a
Complete List of Authors:	Gleeson, Duangkamol; King Mongkut's Institute of Technology Ladkrabang, Chemistry

**SCHOLARONE™**  
Manuscripts

1  
2  
3  
4     SKELETAL ISOMERIZATION OF BUTENE IN FERRIERI  
5  
6  
7     THE ENERGETIC AND STRUCTURAL DIFFERENCES BE  
8  
9  
10  
11  
12     AND ALKOXIDE BASED PATHWAYS.  
13  
14  
15  
16  
17

18                     *Duangkamol Gleeson*<sup>1\*</sup>  
19  
20  
21  
22  
23  
24     <sup>1</sup> DEPARTMENT OF CHEMISTRY, FACULTY OF SCIENCE, KING MONGKUT'S INSTITUTE OF TECHN  
25  
26                     BANGKOK 10520, THAILAND  
27  
28  
29  
30  
31  
32  
33  
34                     EMAIL: [KTDUANGK@KMITL.AC.TH](mailto:KTDUANGK@KMITL.AC.TH)  
35  
36  
37                     \*CORRESPONDING AUTHOR: TEL: +6623298400 EXTN. 6231, FAX: +6623298428  
38  
39  
40  
41  
42     KEYWORDS: SKELETAL ISOMERIZATION, ZEOLITE CATALYSIS, BUTENE, DFT, M06-2X, FF  
43  
44  
45  
46  
47  
48  
49  
50  
51  
52  
53  
54  
55  
56  
57  
58  
59  
60

**Abstract**

1  
2  
3 IN THIS STUDY THE RESULTS FROM A SYSTEMATIC ANALYSIS OF TWO DIFFERENT MECH-  
4 ISOMERISATION OF CIS-BUTENE TO ISO-BUTENE IN FERRIERITE ARE PRESENTED. ONE INVOLVES  
5 THAT PROCEEDS VIA STABLE ALKOXIDE INTERMEDIATES AND THE OTHER IS ONE WHICH PROCE-  
6 DURES VIA CARBENIUM ION INTERMEDIATES. A 27T QM CLUSTER MODEL HAS BEEN USED HERE FOR  
7 THIS PURPOSE, WHICH IS DESCRIBED USING THE B3LYP DENSITY FUNCTIONAL. ALTHOUGH THE CARBENIUM  
8 ION STRUCTURES FORMED OVER THE PATHWAY ARE STABLER THAN THE ALKOXIDE INTERMEDIATES,  
9 THE ALKOXIDE INTERMEDIATES FORMED IN THE CONVENTIONAL MECHANISM, THE RATE DETER-  
10 MING THE ISOMERISATION IS APPROXIMATELY 1000 TIMES FASTER THAN THE CARBENIUM  
11 ION BASED MECHANISM. THE HIGHER BARRIER FOR THE LATTER PROCE-  
12 DURE IS DUE TO THE STABILITY OF THE INTERMEDIATES FORMED WITHIN THE PORE. THIS APPEARS TO SUGGEST THAT  
13 THE ALKOXIDE INTERMEDIATES ARE FORMED OVER THE COURSE OF A REACTION, THE SKELETAL ISOMERISATION OF BUTENE  
14 IS A CARBENIUM BASED MECHANISM. THIS PROPOSAL IS CONSISTENT WITH EXPERIMENTAL  
15 OBSERVATIONS THAT THE ALKOXIDE INTERMEDIATES ARE EXPERIMENTALLY OBSERVED SPECIES.

16  
17  
18  
19  
20  
21  
22  
23  
24  
25  
26  
27  
28  
29  
30  
31  
32  
33  
34  
35  
36  
37  
38  
39  
40  
41  
42  
43  
44  
45  
46  
47  
48  
49  
50  
51  
52  
53  
54  
55  
56  
57  
58  
59  
60

## 1.0 Introduction

1  
2 ZEOLITES ARE IMPORTANT SILICON BASED CATALYSTS EMPLOYED IN THE PETROCHEMICAL  
3  
4 MATERIALS INTO REFINED<sup>2</sup> PREDE~~DE~~IRABLE CATALYTIC ACTIVITY OF THESE MATERIALS MAINLY  
5  
6 THE REPLACEMENT OF INDIVIDUAL SILICON ATOMS IN THE 3D LATTICE STRUCTURE WITH ALUMINA  
7  
8 ACIDIC CENTER AND/OR (B) THE PRESENCE OF ADDITIONAL HEAVY METALS<sup>25</sup> COMBINING WITH THE  
9  
10 DIVERSE RANGE OF THREE DIMENSIONAL PORE STRUCTURES THAT<sup>26</sup> SURANGA TER USES EXHIBIT  
11  
12 REACTIONS CAN BE CATALYZED BY THESE<sup>10</sup> EXCHANGES WHERE SUCH MATERIALS HAVE  
13  
14 PARTICULARLY USEFUL IS IN THE CATALYTIC CRACKING AND SKELETAL ISOMERISATION OF  
15  
16 PETROCHEMICAL INDUSTRY<sup>11</sup> THE SKELETAL ISOMERISATION OF LINEAR BUTENES TO<sup>12</sup> ISOBUTENE  
17  
18 EXTENSIVELY STUDIED EXPERIMENTALLY<sup>13</sup> THAT THE LATTER IS AN IMPORTANT<sup>14</sup> CHEMICAL PRECURSOR  
19  
20 IN THIS STUDY THE RELATED CATALYTIC CONVERSION OF CIS-BUTENE TO ISO-BUTENE IN THE  
21  
22 INVESTIGATED. THIS ZEOLITE IS OF SIGNIFICANT INTEREST FROM THE POINT OF VIEW OF BUTENE  
23  
24 HIGH SELECTIVITY IT DISPLAYS FOR ISO-BUTENE COMPARED TO LARGER PORE<sup>20</sup> ZEOLITES<sup>21</sup> S  
25  
26 DIFFERENCES ARISE DUE TO THE SO CALLED CONFINEMENT EFFECT OF THE UNIQUE ZEOLITE  
27  
28 ACIDITY<sup>6</sup> THERE ARE STILL A NUMBER OF UNCERTAINTIES REGARDING THE ORIGIN OF THE CATALYTIC  
29  
30 THIS REACTION, INCLUDING WHETHER IT OCCURS VIA A MONO-MOLECULAR<sup>7</sup> OR PSEUDO BI-MOLECULAR<sup>8</sup>  
31  
32 EXTENSIVE EXPERIMENTATION HAS BEEN UNDERTAKEN ON ZEOLITES USING TECHNIQUES SUCH  
33  
34 AS<sup>15</sup> NMR SPECTROSCOPY<sup>16</sup> IN ADDITION EXTENSIVE USE OF THEORETICAL METHODS HAVE BEEN  
35  
36 LITERATURE. QUANTUM MECHANICAL (QM) CALCULATIONS OF VARIOUS TYPES HAVE BEEN EMPLOYED  
37  
38 OF ZEOLITE CATALYSIS INCLUDING QM CLUSTER<sup>12</sup>,<sup>25</sup> C<sup>13</sup> DFT QM<sup>14</sup> QUANTUM MECHANICAL/MOLECULAR  
39  
40 MECHANICAL (QM/MM)<sup>14</sup> AND ONIOM METHODS<sup>17</sup> AS WELL AS PERIODIC DFT SIMULATIONS<sup>20</sup> STUDY,  
41  
42 A RELATIVELY LARGE DFT CLUSTER MODEL OF FER IS EMPLOYED TO STUDY THE LOCAL EFFECTS  
43  
44 THE SKELETAL ISOMERISATION OF CIS-BUTENE IN THE ZEOLITE (FIGURE 1) SINCE REPORTS FROM  
45  
46 SUCH A SIZED CLUSTER IS NEEDED TO ENABLE THE LOCATIONS OF HIGH ENERGY<sup>32</sup> CARBENIUM  
47  
48 IMPROVED M062X DFT FUNCTIONAL<sup>22</sup> EMPLOYED HERE AS IT HAS BEEN USED QUITE EXTENSIVELY<sup>23</sup> IN  
49  
50 OF ZEOLITE CATALYSIS RECENTLY<sup>7</sup><sup>12</sup><sup>28</sup><sup>25</sup>

1 THE INVESTIGATIONS OF BORONATEE MEDIUM PORE ZEOLITE THETA-1 SHOWED THAT  
2 ISOMERISATION REACTION OF LINEAR BUTENES PROCEEDS VIA TWO ALKOXIDE INTERMEDIA  
3 BUTYL) TO THE ISO-BUTENE PRODUCT. THE RATE DETERMINING BARRIER IS 22 KCAL/MOL A  
4 MIGRATION. NO CARBENIUM ION STATIONARY POINTS WERE REPORTED IN THETA-1 OR <sup>37</sup> FER BY A RE  
5 THIS AUTHOR. DEMUTH ET AL INVESTIGATED THE RELATED SKELETAL ISOMERISATION OF 2-PE  
6 THE MOST LIKELY PATHWAY INVOLVED THE FORMATION OF HIGH ENERGY, BUT STABLE SEC  
7 TRANSIENT INTERMED~~I~~<sup>38</sup> DIFFERING RESULT MAY BE DUE TO DIFFERENCES IN THE ZEOLITE PO  
8 INVESTIGATION IN THE DIFFERENT STUDIES SINCE THESE ARE KNOWN TO HAVE A DRAMATIC  
9 CARBENIUM <sup>39,40</sup> IONS NIEMENAN <sup>41</sup> HAS ALSO ASSESSED ASPECTS OF ALKOXIDE SPECIES STABILITI  
10 ALKENES BETWEEN 3 TO 5 CARBONS IN LENGTH. THEY SHOWED THAT THE STABILITY OF THE  
11 SENSITIVE TO THE STERIC BULK OF THE ALKENE IN QUESTION. IN ADDITION, A NUMBER OF S  
12 IMPORTANCE OF CARBENIUM IONS AND THEIR RELEVANCE IN SKELETAL ISOMERISATION OF  
13 AL<sup>42,43</sup>, FOLLOWED BY BORONATE CONCLUDED THAT CARBENIUM IONS SHOULD EXIST AS TRUE, A  
14 REACTION INTERMEDIATES.

15 THIS STUDY CONSIDERS THE SKELETAL ISOMERISATION OF LINEAR BUTENES TO ISO-BUTENE I  
16 RECENT PUBLICATIONS IN THE AREA. BOTH A CONVENTIONAL MECHANISM AKN TO <sup>36,40</sup> THAT PRO  
17 THAT PROCEEDS VIA ALKOXIDE INTERMEDIATES, AND ONE THAT PROCEEDS VIA <sup>39</sup> CARBENIUM  
18 INVESTIGATED. THE ZEOLITE FER HAS BEEN CHOSEN FOR THIS STUDY DUE TO ITS WIDE  
19 ISOMERISATION REACTIONS(B) DUE TO ITS RATHER SMALL PORE CAVITY WHICH PRESUMABLY  
20 ION FORMATION MORE LIKELY WHEN COMPARED TO LARGER PORE ZEOLITES SUCH AS ZSM  
21 CONTRASTED WITH RELATED THEORETICAL STUDIES WHICH HAVE BEEN PERFORMED IN EITHE  
22 SIMILAR ALKENES: <sup>40</sup> ZSM-22<sup>36,38</sup>, ZSM-5<sup>37</sup> AND FER<sup>38,41,42</sup> OR GENERIC ZEOLITE<sup>45</sup> MODELS

## 55 2.0 Models and Methods

56 RECENT CALCULATIONS ON FER HAVE USED THE CLUSTER APPROACH<sup>38</sup> AND PERIODIC  
57 METHODS<sup>43,46</sup> TO GOOD EFFECT TO ELUCIDATE ASPECTS OF ITS CATALYTIC FUNCTION. DUE TO THE  
58 CLUSTER APPROACH, AND THE ABILITY OF RELATIVELY LARGE CLUSTERS TO DESCRIBE HIGH  
59

1 WITHIN ZEOLITE SYSTEMS CLUSTER METHOD WAS CHOSEN FOR THIS STUDY. THE CLUSTER M  
2 GENERATED USING THE X-RAY DIFFRACTION DATA<sup>47</sup> IN A 3D CUBICAL 10 T  
3 A LARGE MAIN 10T CHANNEL BISECTED BY SMALLER 8T CHANNELS. A 27T CLUSTER MODEL WAS  
4 COORDINATES, ENCOMPASSING 2 COMPLETE PORES EITHER SIDE OF THE 10T CENTRAL RING. TH  
5 CREATED BY REPLACING A SILICON ATOM LOCATED AT THE T2 POSITION OF THE 10T<sup>74</sup> RING WITH  
6 THE 6T REGION OF THE CLUSTER MODEL SURROUNDING THE T2 SITE AND ACIDIC OXYGEN US  
7 AND MORE DISTANT ATOMS USING THE 3-21G BASIS SET (FIGURE 1). THIS APPROACH HAS BEEN  
8 ALLOW A LARGE QM CLUSTER OF A ZEOLITE TO BE SIMULATED IN A REASONABLE BASIS SET OF T  
9 DOES APPEAR TO BE SUFFICIENT TO DESCRIBE LONGER RANGE EFFECTS BASED ON<sup>48,49</sup> THIS REPO  
10 RESULTED IN A MODEL SYSTEM WITH A TOTAL OF 1226 BASIS FUNCTIONS.

11 THE 6T REGION SURROUNDING THE T2 SITE AND ACIDIC OXYGEN WAS EXCISED FROM THE ORI  
12 WITH BONDS CUT ACROSS THE O-SI BOND. TO AVOID ISSUES DUE TO OVERLY STRONG POLARIZA  
13 OH GROUPS, BONDS WERE CUT ACROSS THE SI-O BONDS FOR THE MORE<sup>46</sup> REMAINING OF AT  
14 APPROACH IS SIMILAR TO THAT EMPLOYED TO ZHAO ET AL IN THEIR VALIDATION OF THE M0  
15 BASED APPLICATION<sup>35</sup> TO MAINTAIN THE OVERALL SHAPE OF THE ZEOLITE ALL TERMINAL HYDRO  
16 REGION WERE FIXED WHILE ONLY SILICON ATOMS BEYOND THIS REGION WERE FIXED. THIS ALLO  
17 OXYGEN ATOMS, WHICH ARE DIRECTED INTO THE FER PORE, TO SUBTLY ALTER THEIR POSITION  
18 SIMULATED REACTION, THEREBY ALLOWING BETTER STABILIZATION OF THE REACTIVE SPECIE  
19 THAT THE LACK OF FLEXIBILITY IN THE ZEOLITE LATTICE IS ONE OF THE KEY ISSUES IN E  
20 INTERMEDIATES IN QM MODELS<sup>49</sup> OF ZEOLITES

21 ALL GEOMETRY OPTIMIZATIONS WERE PERFORMED USING M06-2X FUNCTIONAL<sup>50</sup> WITH GAUSSIAN  
22 THE MINNESOTA DENSITY FUNCTIONALS MODULE 3.1 BY<sup>32</sup> ZHAI AND AND HAN TRANSITION STATES  
23 FULLY CHARACTERIZED AS STATIONARY POINTS IN THE COMPLETE 27T MODEL, IN ALL CASES  
24 SINGLE NEGATIVE FREQUENTLY, RESPECTIVELY. ZERO POINT ENERGY CORRECTIONS TO THE  
25 POSSIBLE. SINGLE POINT ENERGIES OF OPTIMIZED COORDINATES WERE SUBSEQUENTLY OBT  
26 FUNCTIONAL WITH THE 6-311+G(2DF,DP) BASIS SET USED FOR THE 6T REGION AND 6-31G\* FOR THE

1 WITH REGARDS TO MODEL VALIDITY, THE SKELETAL ISOMERIZATION OF LINEAR BUTENES  
2 BEEN STUDIED BY BORONAT ET AL IN THETA-1 USING A 20T MODEL. THE OF THE REPORTED THAT  
3 RESULTS WERE IN AGREEMENT WITH PERIODIC MODELS THAT INCLUDE LONGER RANGE EFFECTS.  
4 THIS FINDING SHOULD MEAN THAT THE RESULTS OBTAINED HERE FROM A LARGER 27T MODEL  
5 WITH REASONABLE ACCURACY.

### 14 3.0 Results and Discussion

15 THE ENERGETIC RESULTS OBTAINED FROM THE CALCULATIONS ARE REPORTED IN TABLE 1 AND  
16 THE PARAMETERS OF THE OPTIMIZED GEOMETRIES ARE DISPLAYED IN FIGURE 2 FOR MINIMA AND  
17 MAXIMA STATES. THE ENERGIES OF THE OPTIMIZED COMPLEXES ARE GIVEN IN TABLE 2 ALONG WITH THE  
18 POINT CORRECTION AND THE SINGLE POINT ENERGIES. THE SINGLE POINT AND ZPE CORRECTIONS  
19 ARE IN GOOD AGREEMENT WITH THE ENERGIES OBTAINED AT THE ORIGINAL LEVEL OR THEORETICALLY  
20 HENCEFORTH CORRESPOND TO THE SINGLE POINT ENERGIES (M062X WITH 6-311+G(2DF,DP) FOR C  
21 REGION AND 6-31G(D) FOR 21T REGION) INCLUDING ZERO POINT ENERGY CORRECTIONS, AND ARE  
22 THE ISOLATED REAGENTS UNLESS OTHERWISE STATED.

23 THE SKELETAL ISOMERISATION OF CIS-BUTENE IS FIRST DISCUSSED IN THE CONTEXT OF THE MECHANISM  
24 BASED MECHANISM FOLLOWED BY A DISCUSSION ON THE RELATIVE LIKELIHOOD OF A CARBENE  
25 EXISTING IN THIS ZEOLITE.

#### 45 3.1 Alkoxide based mechanism

46 THE TRADITIONAL UNI-MOLECULAR MECHANISM OF BUTENE ISOMERISATION BEGINS WITH THE  
47 ADSORBED ALKENE-FER COMPLEX. THE ESTIMATED ADSORPTION ENERGY OF 1-BUTENE IS -18.9  
48 KCAL/MOL AND -18.4 KCAL/MOL FOR ISO-BUTENE. THE VALUE OF -23.8 KCAL/MOL OBTAINED HERE FOR  
49 THE FER COMPLEX DISPLAYS SHORT C---H INTERACTIONS AS EXPECTED WHILE THE C---C BOND DISTANCE  
50 IS ONLY SLIGHTLY ELONGATED COMPARED TO THE ISOLATED GAS PHASE VALUE (1.34 VS 1.33 Å).

1 THE SKELETAL ISOMERISATION IN THETA-1 BEGINS WITH THE FORMATION OF A SECONDARY  
2 CONCERTED MECHANISM WITH SIMULTANEOUS TRANSFER OF A PROTON FROM THE ZEOLITE TO  
3 A C-O BOND<sup>36,40</sup>. THE NEXT STEP REQUIRES A METHYL GROUP SHIFT, LEADING TO THE FORMATION  
4 OF AN INTERMEDIATE. THE CARBON ATOM FROM WHICH THE METHYL GROUP MIGRATES FORMS A C-  
5 NUCLEOPHILIC OXYGEN, WHILE THE MIGRATING METHYL SATISFIES THE VALENCE OF THE CARBON.  
6 MUST BREAK. THE SECONDARY ALKOXIDE IS FOUND TO BE 6.9 KCAL/MOL HIGHER IN ENERGY THAN  
7 COMPARED TO THE PRIMARY ALKOXIDE WHICH IS -2.9 KCAL/MOL LOWER. THE RATE DETERMINING  
8 DECOMPOSITION OF THE PRIMARY ALKOXIDE TO GIVE ADSORBED ISO-BUTENE. THIS FINAL STEP  
9 DECOMPOSES THE PRIMARY ALKOXIDE TO BREAK AND THE TRANSFER OF A PROTON TO THE ZEOLITE WHICH  
10 OF 32.7 KCAL/MOL. ISO-BUTENE IS FOUND TO BE ADSORBED TO THETA-1 ONLY 0.7 KCAL/MOL HIGHER  
11 THAN BUTENE. BORONAT ET AL NOTE THAT THESE ENERGIES ARE LIKELY TO BE UPPER LIMITS GIVEN  
12 THAT THE 5T OPTIMIZED MODEL WAS INSERTED INTO THE LARGER MODEL AND A SINGLE POINT  
13 PERFORMANCE<sup>26</sup>)

14 IN FER, IT IS FOUND THAT THE FORMATION OF THE INITIAL ALKOXIDE INTERMEDIATE DOES  
15 MANNER, IN CONTRAST TO THAN WITHIN THETHETA-1 PORE. PROTON TRANSFER FROM THE O2 AND  
16 OF CIS-BUTENE VIA TRANSITION STATE ONE (TS1) LEADS TO A STABLE CARBENIUM ION 18.3 KCAL/MOL  
17 THAN THE ADSORBED COMPLEX, WITH A BARRIER OF 19.9 KCAL/MOL. THE C2-C3 DISTANCE OF 1.54 Å  
18 INCREASES TO 1.61 Å IN CARBENIUM ION 1 (CARB1), INTERMEDIATE BETWEEN THE DOUBLE AND SINGLE  
19 BOND. THE C2-C3 DISTANCE OF 1.54 Å IS EXPECTED FOR CIS-BUTENE IN THE GASPHASE<sup>41</sup> (RESPECTIVELY). TS1 IS CONSIDERABLY CLOSER IN  
20 TO THE CORRESPONDING CARBENIUM ION THAN ADSORBED CIS-BUTENE AS MIGHT BE EXPECTED  
21 DIFFERENCES. TS1 HAS A C2-C3 DISTANCE THAT IS VERY CLOSE TO THAT OF CARB1 (1.61 Å) AND THE  
22 C2-HZ DISTANCE OF (1.14 VS 1.13 Å). THE PRINCIPAL DIFFERENCE BEING THE TWO IS THE C1-C2-C3-C4  
23 ANGLE, WHICH IS 107° IN CARB1 BUT 114° IN TS1, FACILITATING THE INDUCTIVE STABILIZATION OF THE  
24 CHARGED CARBON CENTER IN THE FORMER. CARB1 IS STABILIZED BY A SINGLE STRONG INTERACTION  
25 C4 HYDROGEN ATOM AND THE O3 OXYGEN<sup>42</sup> AS IS SIMILARLY TO THOSE REPORTED BY FANG ET AL.  
26 CARB1 CAN DECOMPOSE IN THE FORWARD DIRECTION TO A SECONDARY ALKOXIDE INTERMEDIATE  
27 BARRIER OF JUST 1.2 KCAL/MOL. THE C3-O1 DISTANCE IS INCREASING TO 1.56 Å IN THE ALKOXIDE

1 INTERMEDIATE (INT1). THIS STRUCTURE IS ~ 1 KCAL/MOL LOWER IN ENERGY THAN THE ADSORBED  
2 THAT REPORTED BY BORONAT ET AL IN THETA-1 (6.9 KCAL/MOL). THIS DIFFERENCE IS NOT SURPRISING  
3 AUTHORS SHOW THAT ALKOXIDES FORMED IN MORDENITE WERE SHOWN TO BE HEAVILY DEPENDENT  
4  
5 DO OTHERS  
6  
7  
8

9 INTERMEDIATE 2 (INT2) IS FORMED WHEN THE METHYL GROUP (C1) MIGRATES FROM C2 TO C3.  
10 O1-C3 BOND TO BREAK AND THE O1-C2 BOND TO FORM IN THE PROCESS. THE TRANSITION STATE  
11 C2=C3 DOUBLE BOND AS OBSERVED BY ~~WORKHORDE~~ IS THE 0.93-C1 DISTANCE AS WHILE THE C2-O2  
12  
13  
14  
15  
16  
17  
18  
19  
20  
21  
22  
23  
24  
25  
26  
27  
28  
29  
30  
31  
32  
33  
34  
35  
36  
37  
38  
39  
40  
41  
42  
43  
44  
45  
46  
47  
48  
49  
50  
51  
52  
53  
54  
55  
56  
57  
58  
59  
60

INTERMEDIATE 2 (INT2) IS FORMED WHEN THE METHYL GROUP (C1) MIGRATES FROM C2 TO C3.  
O1-C3 BOND TO BREAK AND THE O1-C2 BOND TO FORM IN THE PROCESS. THE TRANSITION STATE  
C2=C3 DOUBLE BOND AS OBSERVED BY ~~WORKHORDE~~ IS THE 0.93-C1 DISTANCE AS WHILE THE C2-O2  
BETWEEN THESE TWO ATOMS. THE C1-C2 DISTANCE AND THE O2-C1 DISTANCE AS WHILE THE C2-O2  
AND O1-C3 DISTANCES ARE AND 2.9 Å RESPECTIVELY. THE BARRIER OF 24 KCAL/MOL IS CONSISTENT  
OBSERVED BY BORONAT ET AL IN THETA-1 (25.8 KCAL/MOL). THE SECONDARY ALKOXIDE IS 2 KCAL/MOL  
HIGHER THAN THE ADSORBED ISOBUTENE IN FER FROM THE WORKHORDE. THIS IS CONSISTENT WITH WHAT IS  
HERE (2.5 KCAL/MOL).

TS5 SEPARATES INT2 FROM CARBENIUM ION 3, AND NOT THE PRODUCT AS IS FOUND IN THETA-1.  
O2-C2 BOND SEES THE MIGRATION OF THE HYDROGEN ATOM ATTACHED TO C3 TO C2 AS THE  
FORM. PROTON TRANSFER FROM THIS TERTIARY CENTER TO THE ZEOLITE WAS NOT OBSERVED.  
PRIMARY CARBENIUM CENTER THAT FORMS AT C2. TS5 THEREFORE DISPLAYS THE C2-C3 DISTANCE AS  
DISTANCE IS Å. THE C2-C3 DISTANCE IS Å. CRUCIALLY, THE C2-C3-H ANGLE IS °, INDICATING THAT THE  
PROTON IS IN THE PROCESS OF MIGRATING ACROSS THE C2-C3 BOND. THIS FINDING IS CONSISTENT  
CARBENIUM IONS ARE DEPENDENT ON THE ACCESSIBILITY OF THE ACIDIC SITES AND REACTIONS  
COMPARABLE TO THE FINAL RATE DETERMINING STEP FOUND BY BORONAT ET AL IN THETA-1 (3.8 KCAL/MOL).

THE TERTIARY BUTYL CARBENIUM ION (CARB3) DISPLAYS C-C DISTANCES OF APPROXIMATELY 2.7 Å AND 2.9 Å.  
UNIQUE PORE DIMENSIONS, THE TERTIARY BUTYL CARBENIUM ION CAN MAKE SIGNIFICANT INTERACTIONS WITH THE  
IN FACT, ALL 9 HYDROGEN ATOMS ARE FOUND TO MAKE SIGNIFICANT INTERACTIONS WITH THE  
-O INTERACTIONS OBSERVED (ONE PER ALKYL). THE C-C DISTANCES ARE 2.7 Å AND 2.9 Å (FIGURE 6), WHICH  
WOULD EXPLAIN THE VERY LOW NET CHANGE ON THE MOLECULE COMPARED TO CARB1 (FIGURE 5), WHICH  
DISCUSSED IN MORE DETAIL IN THE FOLLOWING SECTION.

1 CARB3 IS FOUND TO BE 6 KCAL/MOL HIGHER IN ENERGY THAN THE ADSORBED CIS-BUTENE AND  
2 THE LATTER ENERGY IS LOWER THAN THE VALUE REPORTED VERY RECENTLY BY TUMA ET AL.  
3 CARBENIUM – ADSORBED ISO-BUTENE IS CLOSER TO THEIR EARLIER REPORTED VALUE OF 15 KCAL/MOL.  
4  
5 AL ALSO REPORT THAT THE TERTIARY BUTYL CARBENIUM ION IS 14.7 KCAL/MOL HIGHER IN ENERGY  
6 ISO-BUTENE MOLECULES IN ZSM5. HOWEVER, IN THIS CASE THE LARGER 12T PORE OF ZSM5 IS UNKNOWN  
7 SAME LEVEL OF STABILIZATION TO THE CARBENIUM ION OF THE SMALLER FER PORE AS DISCUSSED.  
8  
9 TRANSITION STATE 7 (TS7) CONNECTS CARB3 WITH THE ADSORBED ISO-BUTENE MOLECULE. THE  
10 TS7 IS 1.36 Å, THE O2-HZ DISTANCE IS FOUND TO BE 1.35 Å. THE C1-C3 DISTANCE IS THE BARRIER TO  
11 REACTION IS CONSIDERABLY HIGHER THAN THAT OBSERVED FOR CARB1 DUE TO THE INHERENT  
12 THE STABILIZATION PROVIDED BY THE ZEOLITE LEADS TO A FORWARD BARRIER TO REACTION OF 12 KCAL/MOL  
13 IN THE REVERSE DIRECTION). THIS VALUE IS SOMEWHAT HIGHER THAN IN THE SIMILAR STUDY OF 11 KCAL/MOL  
14 IN FER (3.3 KCAL/MOL) REPORTED BY TUMA ET AL. THIS BE A REFLECTION OF THE DIFFERENT  
15 METHODOLOGIES USED.

16 THE ADSORBED ISO-BUTENE MOLECULE IS OF EQUIVALENT ENERGY TO THE ADSORBED CIS-BUTENE  
17 THAT FOUND IN THE FER. LIKE THE ADSORBED CIS-BUTENE MOLECULE, THE INTERACTION BETWEEN  
18 THE ALKENE DOUBLE OF ISO-BUTENE MOLECULE IS NOT APPROXIMATELY SYMMETRIC. IN THE  
19 DISTANCE IS FOUND TO BE 1.35 Å. THE C3---HZ DISTANCE IS 1.65 Å. HOWEVER THE SYMMETRIC NATURE OF THE  
20 BUTENE MOLECULE, AND THE LOCATION OF THE O1 ACIDIC ATOM AT A LESS RESTRICTED PART OF THE  
21 SOMEWHAT POORER INTERACTION OF ISO-BUTENE IS SOMEWHAT COMPENSATED FOR BY REDUCED  
22  
23  
24  
25  
26  
27  
28  
29  
30  
31  
32  
33  
34  
35  
36  
37  
38  
39  
40  
41  
42  
43  
44  
45  
46  
47  
48  
49

### 50 3.2 Carbenium based mechanism

51 THE THE SKELETAL ISOMERISION OF CIS-BUTENE TO ISO-BUTENE CAN PROCEED IN A MANNER  
52 REPORTED TO BORONAT ET AL IN THETA-1. THE KEY DIFFERENCE IS THAT THE VERY FIRST, AND  
53 REPORTED TO BE CONCERTED IN THETA-1, ARE FOUND TO BE STEPWISE IN FER, INVOLVING 2  
54  
55  
56  
57  
58  
59  
60  
61  
62  
63  
64  
65  
66  
67  
68  
69  
70  
71  
72  
73  
74  
75  
76  
77  
78  
79  
80  
81  
82  
83  
84  
85  
86  
87  
88  
89  
90  
91  
92  
93  
94  
95  
96  
97  
98  
99  
100  
101  
102  
103  
104  
105  
106  
107  
108  
109  
110  
111  
112  
113  
114  
115  
116  
117  
118  
119  
120  
121  
122  
123  
124  
125  
126  
127  
128  
129  
130  
131  
132  
133  
134  
135  
136  
137  
138  
139  
140  
141  
142  
143  
144  
145  
146  
147  
148  
149  
150  
151  
152  
153  
154  
155  
156  
157  
158  
159  
160  
161  
162  
163  
164  
165  
166  
167  
168  
169  
170  
171  
172  
173  
174  
175  
176  
177  
178  
179  
180  
181  
182  
183  
184  
185  
186  
187  
188  
189  
190  
191  
192  
193  
194  
195  
196  
197  
198  
199  
200  
201  
202  
203  
204  
205  
206  
207  
208  
209  
210  
211  
212  
213  
214  
215  
216  
217  
218  
219  
220  
221  
222  
223  
224  
225  
226  
227  
228  
229  
230  
231  
232  
233  
234  
235  
236  
237  
238  
239  
240  
241  
242  
243  
244  
245  
246  
247  
248  
249  
250  
251  
252  
253  
254  
255  
256  
257  
258  
259  
260  
261  
262  
263  
264  
265  
266  
267  
268  
269  
270  
271  
272  
273  
274  
275  
276  
277  
278  
279  
280  
281  
282  
283  
284  
285  
286  
287  
288  
289  
290  
291  
292  
293  
294  
295  
296  
297  
298  
299  
300  
301  
302  
303  
304  
305  
306  
307  
308  
309  
310  
311  
312  
313  
314  
315  
316  
317  
318  
319  
320  
321  
322  
323  
324  
325  
326  
327  
328  
329  
330  
331  
332  
333  
334  
335  
336  
337  
338  
339  
340  
341  
342  
343  
344  
345  
346  
347  
348  
349  
350  
351  
352  
353  
354  
355  
356  
357  
358  
359  
360  
361  
362  
363  
364  
365  
366  
367  
368  
369  
370  
371  
372  
373  
374  
375  
376  
377  
378  
379  
380  
381  
382  
383  
384  
385  
386  
387  
388  
389  
390  
391  
392  
393  
394  
395  
396  
397  
398  
399  
400  
401  
402  
403  
404  
405  
406  
407  
408  
409  
410  
411  
412  
413  
414  
415  
416  
417  
418  
419  
420  
421  
422  
423  
424  
425  
426  
427  
428  
429  
430  
431  
432  
433  
434  
435  
436  
437  
438  
439  
440  
441  
442  
443  
444  
445  
446  
447  
448  
449  
450  
451  
452  
453  
454  
455  
456  
457  
458  
459  
460  
461  
462  
463  
464  
465  
466  
467  
468  
469  
470  
471  
472  
473  
474  
475  
476  
477  
478  
479  
480  
481  
482  
483  
484  
485  
486  
487  
488  
489  
490  
491  
492  
493  
494  
495  
496  
497  
498  
499  
500  
501  
502  
503  
504  
505  
506  
507  
508  
509  
510  
511  
512  
513  
514  
515  
516  
517  
518  
519  
520  
521  
522  
523  
524  
525  
526  
527  
528  
529  
530  
531  
532  
533  
534  
535  
536  
537  
538  
539  
540  
541  
542  
543  
544  
545  
546  
547  
548  
549  
550  
551  
552  
553  
554  
555  
556  
557  
558  
559  
5510  
5511  
5512  
5513  
5514  
5515  
5516  
5517  
5518  
5519  
5520  
5521  
5522  
5523  
5524  
5525  
5526  
5527  
5528  
5529  
5530  
5531  
5532  
5533  
5534  
5535  
5536  
5537  
5538  
5539  
5540  
5541  
5542  
5543  
5544  
5545  
5546  
5547  
5548  
5549  
5550  
5551  
5552  
5553  
5554  
5555  
5556  
5557  
5558  
5559  
55510  
55511  
55512  
55513  
55514  
55515  
55516  
55517  
55518  
55519  
55520  
55521  
55522  
55523  
55524  
55525  
55526  
55527  
55528  
55529  
55530  
55531  
55532  
55533  
55534  
55535  
55536  
55537  
55538  
55539  
55540  
55541  
55542  
55543  
55544  
55545  
55546  
55547  
55548  
55549  
55550  
55551  
55552  
55553  
55554  
55555  
55556  
55557  
55558  
55559  
555510  
555511  
555512  
555513  
555514  
555515  
555516  
555517  
555518  
555519  
555520  
555521  
555522  
555523  
555524  
555525  
555526  
555527  
555528  
555529  
555530  
555531  
555532  
555533  
555534  
555535  
555536  
555537  
555538  
555539  
555540  
555541  
555542  
555543  
555544  
555545  
555546  
555547  
555548  
555549  
555550  
555551  
555552  
555553  
555554  
555555  
555556  
555557  
555558  
555559  
5555510  
5555511  
5555512  
5555513  
5555514  
5555515  
5555516  
5555517  
5555518  
5555519  
5555520  
5555521  
5555522  
5555523  
5555524  
5555525  
5555526  
5555527  
5555528  
5555529  
5555530  
5555531  
5555532  
5555533  
5555534  
5555535  
5555536  
5555537  
5555538  
5555539  
5555540  
5555541  
5555542  
5555543  
5555544  
5555545  
5555546  
5555547  
5555548  
5555549  
5555550  
5555551  
5555552  
5555553  
5555554  
5555555  
5555556  
5555557  
5555558  
5555559  
55555510  
55555511  
55555512  
55555513  
55555514  
55555515  
55555516  
55555517  
55555518  
55555519  
55555520  
55555521  
55555522  
55555523  
55555524  
55555525  
55555526  
55555527  
55555528  
55555529  
55555530  
55555531  
55555532  
55555533  
55555534  
55555535  
55555536  
55555537  
55555538  
55555539  
55555540  
55555541  
55555542  
55555543  
55555544  
55555545  
55555546  
55555547  
55555548  
55555549  
55555550  
55555551  
55555552  
55555553  
55555554  
55555555  
55555556  
55555557  
55555558  
55555559  
555555510  
555555511  
555555512  
555555513  
555555514  
555555515  
555555516  
555555517  
555555518  
555555519  
555555520  
555555521  
555555522  
555555523  
555555524  
555555525  
555555526  
555555527  
555555528  
555555529  
555555530  
555555531  
555555532  
555555533  
555555534  
555555535  
555555536  
555555537  
555555538  
555555539  
555555540  
555555541  
555555542  
555555543  
555555544  
555555545  
555555546  
555555547  
555555548  
555555549  
555555550  
555555551  
555555552  
555555553  
555555554  
555555555  
555555556  
555555557  
555555558  
555555559  
5555555510  
5555555511  
5555555512  
5555555513  
5555555514  
5555555515  
5555555516  
5555555517  
5555555518  
5555555519  
5555555520  
5555555521  
5555555522  
5555555523  
5555555524  
5555555525  
5555555526  
5555555527  
5555555528  
5555555529  
5555555530  
5555555531  
5555555532  
5555555533  
5555555534  
5555555535  
5555555536  
5555555537  
5555555538  
5555555539  
5555555540  
5555555541  
5555555542  
5555555543  
5555555544  
5555555545  
5555555546  
5555555547  
5555555548  
5555555549  
5555555550  
5555555551  
5555555552  
5555555553  
5555555554  
5555555555  
5555555556  
5555555557  
5555555558  
5555555559  
55555555510  
55555555511  
55555555512  
55555555513  
55555555514  
55555555515  
55555555516  
55555555517  
55555555518  
55555555519  
55555555520  
55555555521  
55555555522  
55555555523  
55555555524  
55555555525  
55555555526  
55555555527  
55555555528  
55555555529  
55555555530  
55555555531  
55555555532  
55555555533  
55555555534  
55555555535  
55555555536  
55555555537  
55555555538  
55555555539  
55555555540  
55555555541  
55555555542  
55555555543  
55555555544  
55555555545  
55555555546  
55555555547  
55555555548  
55555555549  
55555555550  
55555555551  
55555555552  
55555555553  
55555555554  
55555555555  
55555555556  
55555555557  
55555555558  
55555555559  
555555555510  
555555555511  
555555555512  
555555555513  
555555555514  
555555555515  
555555555516  
555555555517  
555555555518  
555555555519  
555555555520  
555555555521  
555555555522  
555555555523  
555555555524  
555555555525  
555555555526  
555555555527  
555555555528  
555555555529  
555555555530  
555555555531  
555555555532  
555555555533  
555555555534  
555555555535  
555555555536  
555555555537  
555555555538  
555555555539  
555555555540  
555555555541  
555555555542  
555555555543  
555555555544  
555555555545  
555555555546  
555555555547  
555555555548  
555555555549  
555555555550  
555555555551  
555555555552  
555555555553  
555555555554  
555555555555  
555555555556  
555555555557  
555555555558  
555555555559  
5555555555510  
5555555555511  
5555555555512  
5555555555513  
5555555555514  
5555555555515  
5555555555516  
5555555555517  
5555555555518  
5555555555519  
5555555555520  
5555555555521  
5555555555522  
5555555555523  
5555555555524  
5555555555525  
5555555555526  
5555555555527  
5555555555528  
5555555555529  
5555555555530  
5555555555531  
5555555555532  
5555555555533  
5555555555534  
5555555555535  
5555555555536  
5555555555537  
5555555555538  
5555555555539  
5555555555540  
5555555555541  
5555555555542  
5555555555543  
5555555555544  
5555555555545  
5555555555546  
5555555555547  
5555555555548  
5555555555549  
5555555555550  
5555555555551  
5555555555552  
5555555555553  
5555555555554  
5555555555555  
5555555555556  
5555555555557  
5555555555558  
5555555555559  
55555555555510  
55555555555511  
55555555555512  
55555555555513  
55555555555514  
55555555555515  
55555555555516  
55555555555517  
55555555555518  
55555555555519  
55555555555520  
55555555555521  
55555555555522  
55555555555523  
55555555555524  
55555555555525  
55555555555526  
55555555555527  
55555555555528  
55555555555529  
55555555555530  
55555555555531  
55555555555532  
55555555555533  
55555555555534  
55555555555535  
55555555555536  
55555555555537  
55555555555538  
55555555555539  
55555555555540  
55555555555541  
55555555555542  
55555555555543  
55555555555544  
55555555555545  
55555555555546  
55555555555547  
55555555555548  
55555555555549  
55555555555550  
55555555555551  
55555555555552  
55555555555553  
55555555555554  
55555555555555  
55555555555556  
55555555555557  
55555555555558  
55555555555559  
555555555555510  
555555555555511  
555555555555512  
555555555555513  
555555555555514  
555555555555515  
555555555555516  
555555555555517  
555555555555518  
555555555555519  
555555555555520  
555555555555521  
555555555555522  
555555555555523  
555555555555524  
555555555555525  
555555555555526  
555555555555527  
555555555555528  
555555555555529  
555555555555530  
555555555555531  
555555555555532  
555555555555533  
555555555555534  
555555555555535  
555555555555536  
555555555555537  
555555555555538  
555555555555539  
555555555555540  
555555555555541  
555555555555542  
555555555555543  
555555555555544  
555555555555545  
555555555555546  
555555555555547  
555555555555548  
555555555555549  
555555555555550  
555555555555551  
555555555555552  
555555555555553  
555555555555554  
555555555555555  
555555555555556  
555555555555557  
555555555555558  
555555555555559  
5555555555555510  
5555555555555511  
5555555555555512  
5555555555555513  
5555555555555514  
5555555555555515  
5555555555555516  
5555555555555517  
5555555555555518  
5555555555555519  
5555555555555520  
5555555555555521  
5555555555555522  
5555555555555523  
5555555555555524  
5555555555555525  
5555555555555526  
5555555555555527  
5555555555555528  
5555555555555529  
5555555555555530  
5555555555555531  
5555555555555532  
5555555555555533  
5555555555555534  
5555555555555535  
5555555555555536  
5555555555555537  
5555555555555538  
5555555555555539  
5555555555555540  
5555555555555541  
5555555555555542  
5555555555555543  
5555555555555544  
5555555555555545  
5555555555555546  
5555555555555547  
5555555555555548  
5555555555555549  
5555555555555550  
5555555555555551  
5555555555555552  
555555

1 THE OBSERVATION HERE THAT THE SKELETAL ISOMERISATION OF LINEAR BUTENES IN FER W  
2 FASHION, VIA CARBENIUM ION INTERMEDIATES, IS PERHAPS NOT SURPRISING GIVEN THE RECE  
3 ISO-BUTENE CARBENIUM ION<sup>42</sup> ~~IN FER~~ NOT HOWEVER BEEN REPORTED IF THE SKELETAL ISOM  
4 BUTENES IN FER CAN OCCUR VIA A PURELY CARBENIUM ION BASED PROCESS OR AT LEAST NOW  
5 OR NOT SUCH A MECHANISM WOULD BE IN COMPARISON TO ONE THAT PROCEEDS VIA STABIL  
6 THIS IS NOW DISCUSSED.

7 CARB1, FORMED BY THE TRANSFER OR THE ACIDIC PROTON TO THE C2 ATOM OF CIS-BUTENE, C  
8 ADDITIONAL CARBENIUM ION, TERMED CARB2 HERE. FOR CARB2 TO FORM, THE C1-C2-C3-C4 DIH  
9 ROTATE FROM <sup>0</sup> IN CARB1, TO 44.8° IN THE TRANSITION STATE (TS3), BEFORE REACHING <sup>0</sup> AN MINIM  
10 CARB2. THE BARRIER TO THIS PROCESS IS 4.3 KCAL/MOL. THE MINIMUM ENERGY STRUCT  
11 CORRESPONDING ANGLE ~~AND 41.8~~ 3.2 KCAL/MOL LOWER THAN CARB1 AND 18.3 KCAL/MOL HIGH  
12 THAN THE ADSORBED ISO-BUTENE MOLECULE. IN THIS STRUCTURE THE METHYL GROUP LIES I  
13 AND C3 ATOMS AND IS AKIN TO TS4 DISCUSSED BEFORE. THE KEY DIFFERENCE BETWEEN THE  
14 CARB2 MAKES TWO STRONG INTERACTIONS BETWEEN THE MIGRATING METHYL GROUP AND THE  
15 ATOMS. THE INTERACTIONS OF 2.28 ~~ARE OBSERVED~~ INDICATING THE INTERACTION IS PARTICULAR  
16

17 CARB2 CAN DECOMPOSE TO FORM CARB3\* (RELATED TO CARB3 IN TERMS OF THEIR SYMMETR  
18 THE 001 AXIS IN FER) BY COMPLETING THE MIGRATION OF THE C1 METHYL TO THE C3 POSITION  
19 MIGRATION OF THE C3 HYDROGEN ATOM ACROSS THE C2=C3 BOND AS IT INCREASES IN STRE  
20 GROUP HAS COMPLETELY MIGRATED. THE C3-H DISTANCE<sup>21</sup> C3-H ANGLE IS <sup>0</sup> 99 AND THE C2=C3  
21 DISTANCE IS Å<sup>22</sup> TS6 IS FOUND TO BE HIGHER IN ENERGY THAN THE RELATED TS5 DUE TO THE F  
22 STRUCTURE THE BREAKING C2-O2 BOND (COMING FROM INT2) HELPS STABILIZE THE STRUCTURE  
23 CONSIDERABLY LARGER NET MULLIKEN CHARGE ON THE ALKENE (0.71 VS 0.75 RESPECTIVELY, F  
24

25 CARB3\* IS SLIGHTLY HIGHER IN ENERGY THAN CARB3 (-17.4 VS -18.0 KCAL/MOL). THIS CAN  
26 BASED ON ITS SLIGHTLY REDUCED INTERACTION WITH THE ZEOLITE LATTICE, AS CAN BE SEEN  
27 NET MULLIKEN CHARGE ON THE TWO ALKENES (0.75 VS 0.71 RESPECTIVELY). CARB3\* REACTS  
28 ADSORBED ISO-BUTENE COMPLEX IN A SIMILAR FASHION TO CARB3. THE BARRIER IS FOUND TO  
29 KCAL/MOL HIGHER THAN TS7 WHICH IS ASSOCIATED WITH THE CARB3. AGAIN THE LESS E

PROVIDED BY THE ZEOLITE LATTICE EXPLAINS THE Marginally HIGHER BARRIER BETWEEN (FIGURE 5). THE ADSORBED ISO-BUTENE MOLECULE FROM THIS STEP IS ~3 KCAL/MOL LESS WORKING ARISING FROM THE ALKOXIDE BASED MECHANISM (PRODUCT\*). THESE SUBTLE DIFFERENCES IN THE ACCESSIBILITY OF ATOMS REPORTED BY OTHER RESEARCHERS<sup>28,40,41,51</sup>

THE PREDICTED RATE DETERMINING ENERGY BARRIER FOR THE CARBENIUM ION MEDIATED TRANSFER, CONSIDERABLY LOWER THAN THE 34.2 KCAL/MOL VALUE OBTAINED FOR THE ALKOXIDE EJECTION. THE KEY REASON FOR THE HIGH ENERGY BARRIER IN THE LATTER PROCESS IS THE INHERENT STABILITY OF THE CARBENIUM ION IN ACIDIC ZEOLITES WHICH EXPLAINS WHY THEY ARE EXPERIMENTALLY OBSERVED. IN FER, THE ENERGY BARRIER FOR THE TRANSFER OF THE CARBENIUM ION FROM INT2 TO INT1 IS JUST 27.7 KCAL/MOL, LOWER THAN THE FINAL RATE DETERMINING STEP IN THE EJECTION PROCESS (34.2 KCAL/MOL), SUGGESTING THAT THE FORMATION OF ISO-BUTENE COULD STILL OCCUR ALONG THE ROUTE EVEN THOUGH INT2 IS HIGHLY LIKELY TO FORM GIVEN ITS LOW ENERGY.

1 OXYGEN ATOMS OF THE ZEOLITE LATTICE WHICH CAN LOWER THE OVERALL ENERGY, EVEN  
2 MULLIKEN CHARGES (FIGURE 6). CARB3 AND CARB3\* ARE THE LOWEST IN ENERGY SINCE  
3 CARBENIUM CENTERS, FOLLOWED BY THE SECONDARY CARBENIUM IONS CARB2 AND CARB1.  
4  
5 CARB2 IS LOWER IN ENERGY THAN CARB1 DUE TO THE MORE EFFECTIVE INTERACTIONS IT CAN  
6  
7 LATTICE OXYGEN ATOMS (EVEN THOUGH ITS NET MULLIKEN CHARGE IS HIGHER).  
8  
9

10 THESE RESULTS CONFIRM THE FINDINGS OF OTHERS THAT THE ACCESSIBILITY OF ZEOLITE  
11  
12 DETERMINING THE STABILITY OF INTERMEDIATES AND CARBENIUM IONS FORMED WITH THE  
13  
14 SUGGEST THAT QM MODELS THAT EMPLOY RELATIVELY SMALL FLEXIBLE REGIONS AROUND  
15  
16 EXTENDED ZEOLITE FRAMEWORKS MAY MISS A CONSIDERABLE AMOUNT OF STABILIZATION PRO-  
17  
18  
19  
20  
21  
22  
23  
24 COURSE OF THE REACTION PATHWAYS SIMULATED.  
25  
26  
27  
28  
29

#### 4.0 Conclusions

30 IN THIS STUDY THE RESULTS FROM A SYSTEMATIC ANALYSIS OF TWO DIFFERENT MECH-  
31  
32 ISOMERISTION OF CIS-BUTENE TO ISO-BUTENE HAVE BEEN PRESENTED. ONE INVOLVES A CON-  
33  
34  
35 PROCEEDS VIA STABLE ALKOXIDE INTERMEDIATES AND THE OTHER IS ONE WHICH PROCEEDS VIA  
36  
37  
38 A 27T CLUSTER MODEL HAS BEEN USED HERE FOR THIS PURPOSE USING THE M062X DFT FUNC-  
39  
40 6T REGION HAVE BEEN TREATED USING THE 6-31G(D) BASIS SET AND THOSE IN THE REMAINDE-  
41  
42  
43 USING THE 3-21G BASIS SET. ALL STATIONARY STRUCTURES HAVE BEEN CONFIRMED AS MINIMA  
44  
45  
46  
47  
48  
49  
50  
51  
52  
53  
54  
55  
56  
57  
58  
59  
60  
THE FULL MODEL AND BASIS SET USED FOR OPTIMIZATION. MORE ACCURATE ENERGIES WERE  
POINT ENERGIES (M062X WITH THE 6T REGION TREATED USING 6-311+G(2DF,DP) AND THE RE-  
31G(D)) OF THE OPTIMIZED COORDINATES AND CORRECTING FOR ZERO POINT ENERGY EFFECTS.

THE RESULTS OBTAINED HERE ARE IN GOOD AGREEMENT WITH RELATED REPORTS IN THE LITERA-  
TURE, POSSIBLE, GIVING CONFIDENCE IN THE MODELS USED. THE TRADITIONAL CONCERTED ALK-  
OXIDE MECHANISM IS POSSIBLY THE MECHANISM REPORTED BY BORONATE<sup>36</sup> FOUND IN FER. IN THIS STUDY THE MECHANISM IS FOUND TO  
STEPWISE MANNER WITH PROTON TRANSFER AND NUCLEOPHILIC ATTACK OCCURRING IN SE-  
PAGES

1 RECENT PROPOSALS BY TUMMAHETRAITE DETERMINING STEP FOR THIS MECHANISM IS FOUND TO  
2 (~34 KCAL/MOL) TO THAT REPORTED BY BORONAT ET AL.

3  
4 A PURELY CARBENIUM BASED MECHANISM WAS ALSO INVESTIGATED, WHICH DID NOT REQUIRE  
5 ALKOXIDE INTERMEDIATES. ALTHOUGH THE CARBENIUM ION STRUCTURES FORMED OVER THE  
6  
7 STABLE THAN THE ALKOXIDE INTERMEDIATES FORMED IN THE MORE CONVENTIONAL MECHANISM.  
8  
9 STEP IS PREDICTED TO BE ALMOST 10 KCAL/MOL LOWER IN ENERGY. THE HIGHER BARRIER FOR THE  
10  
11 DUE TO THE INHERENT STABILITY OF THE INTERMEDIATES FORMED WITHIN THE FER PORE. THIS  
12  
13 THESE INTERMEDIATES ARE FORMED OVER THE COURSE OF A REACTION, THE SKELETAL ISOMERISATION  
14  
15 ONLY OCCURS VIA THE CARBENIUM BASED MECHANISM. THIS PROPOSAL IS CONSISTENT WITH THE  
16  
17 ALKOSIDE INTERMEDIATES ARE EXPERIMENTALLY OBSERVED SPECIES.

18  
19 WITH REGARDS TO THE SKELETAL ISOMERISATION OF LINEAR BUTENE IN LARGER ZEOLITES SAWADA  
20  
21 AL REPORT THAT THE TERTIARY BUTYL CARBENIUM ION IS 14 KCAL/MOL HIGHER IN ENERGY  
22  
23 ZEOLITE COMPLEX IS ~8 KCAL/MOL HIGHER IN ENERGY THAN THAT OBSERVED HERE BUT IT IS  
24  
25 CARBENIUM BASED MECHANISM IN ZSM-5 MIGHT BE CLOSE TO ISOENERGETIC WITH THE MORE  
26  
27 BASED MECHANISM. THIS PROPOSAL IS CURRENTLY UNDER INVESTIGATION.

28  
29  
30  
31  
32  
33  
34  
35  
36  
37  
38 **Acknowledgment**  
39

40 THE AUTHOR WOULD LIKE TO THANK PROFESSOR JUMRAS LIMTRAKUL AND DR. PAUL GLEESON  
41  
42 AND CRITICAL INSIGHT DURING THIS STUDY. SHE WOULD ALSO LIKE TO ACKNOWLEDGE FINANCIAL  
43  
44 THAILAND RESEARCH FUND (RMU5180032), THE COMMISSION FOR HIGHER EDUCATION (CHE)  
45  
46 COMPUTATIONAL FACILITIES AT KASETSART UNIVERSITY.  
47  
48  
49  
50  
51  
52  
53  
54  
55  
56  
57  
58  
59  
60

## List of Figures

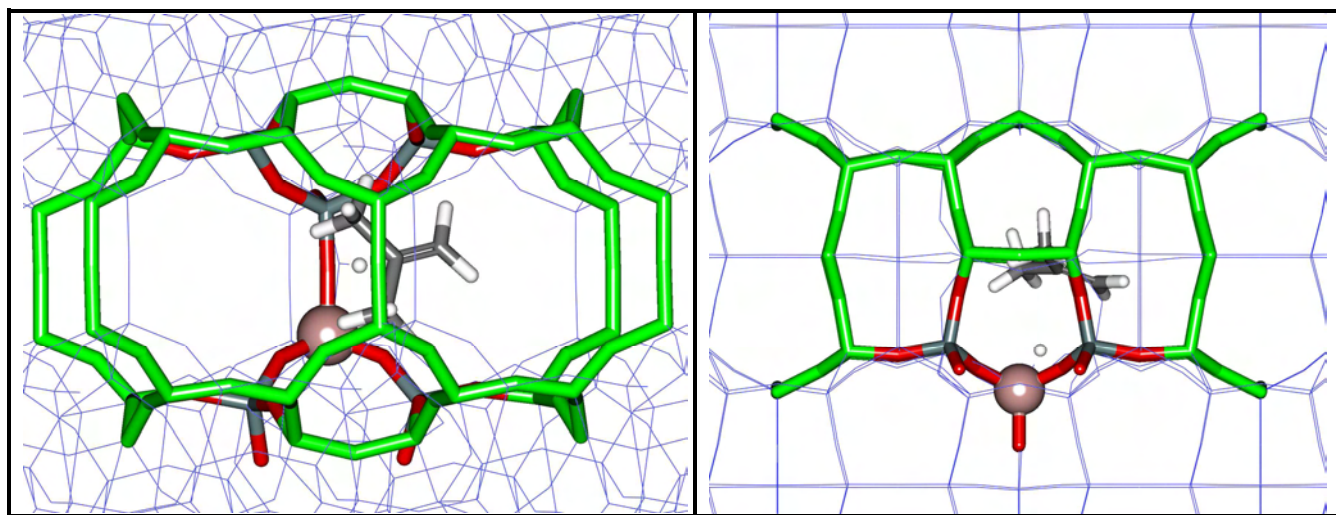


Figure 1 An illustration of the 27T model used in this study (illustrated using a stick representation). The 6T region surrounding the the T2 Al atom and acidic center are described using the 6-31G(d) basis set (O atoms coloured red and Si grey). To include the confinement effect of the zeolite, the two pores that bisect the main 10T ring are also included in the calculation at using the 3-21G basis set (stick representation with all atoms coloured green).

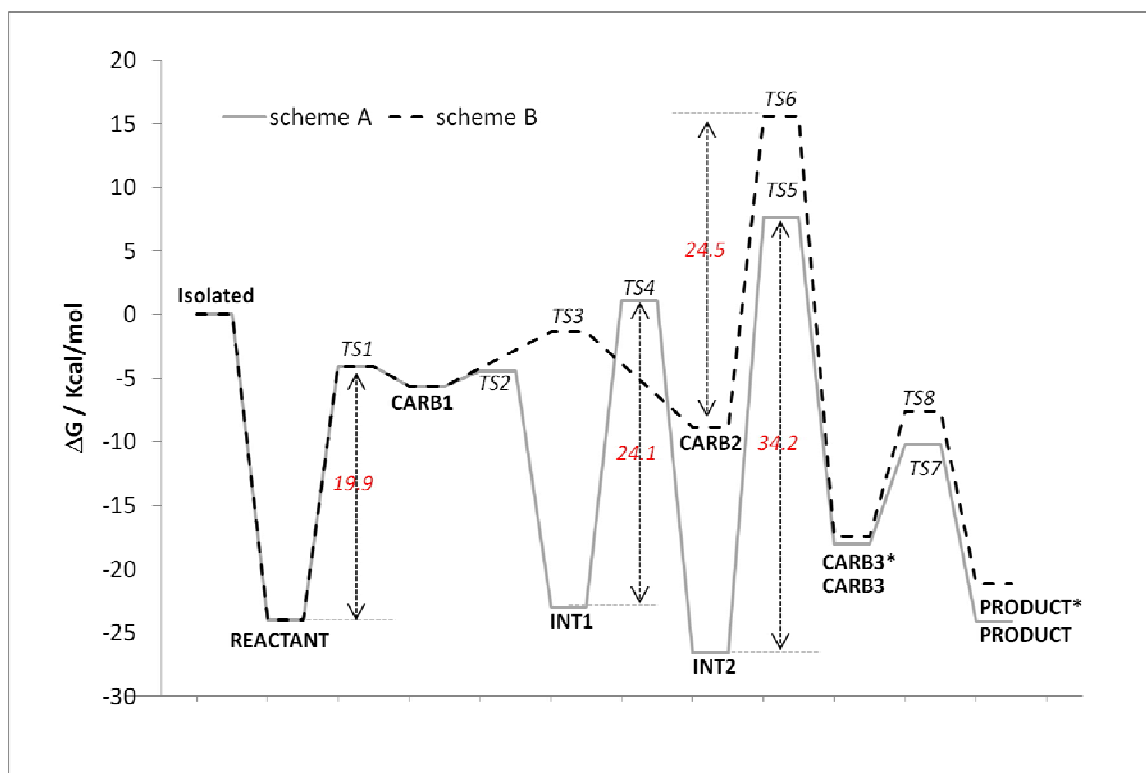


Figure 2 A graphical illustration of the energetic associated with the alkoxide (Scheme A, grey solid line) and carbenium (Scheme B, dashed black line) based mechanisms. The stationary points found on the two pathways are illustrated in Figure 3 and Figure 4.

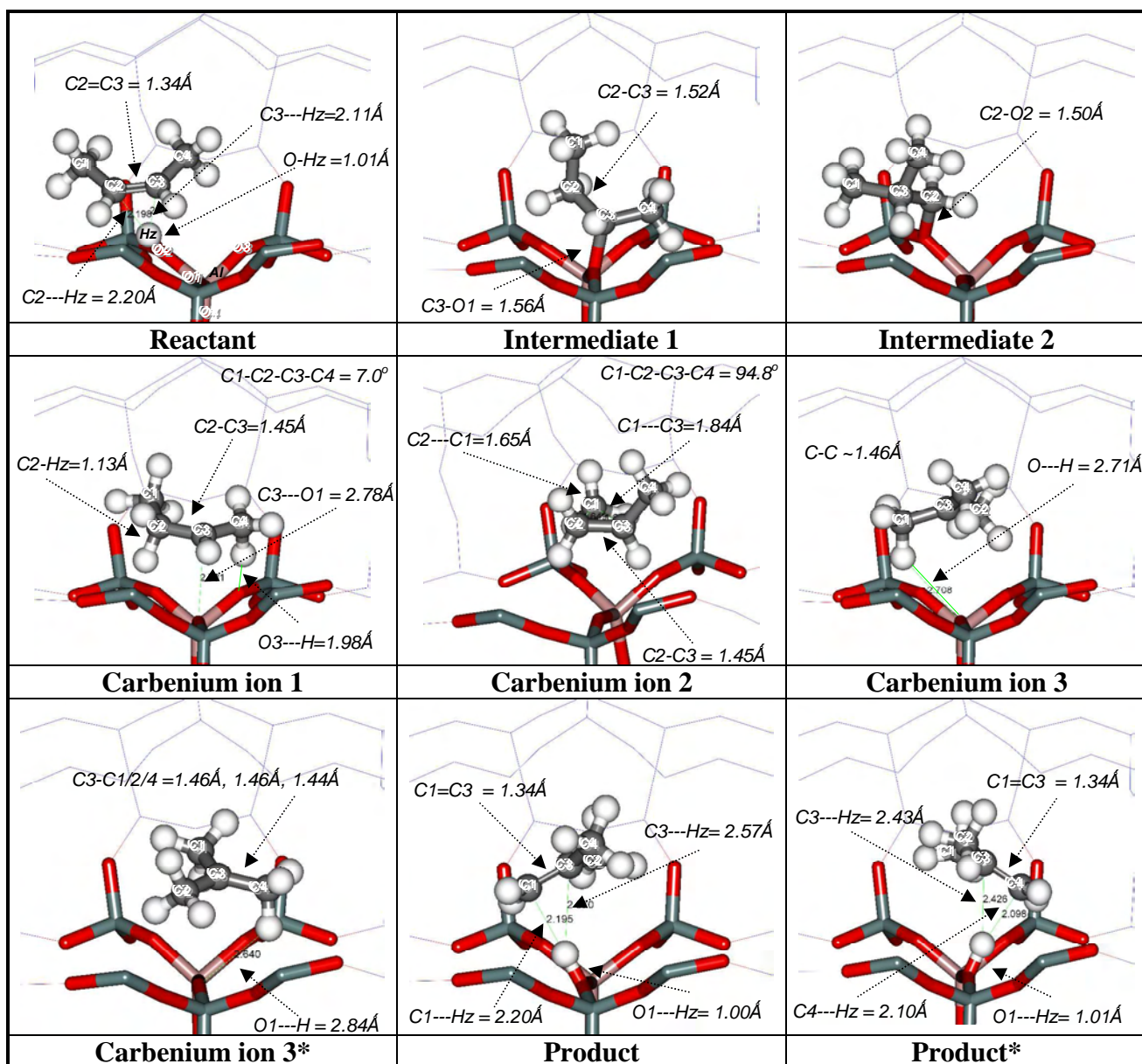
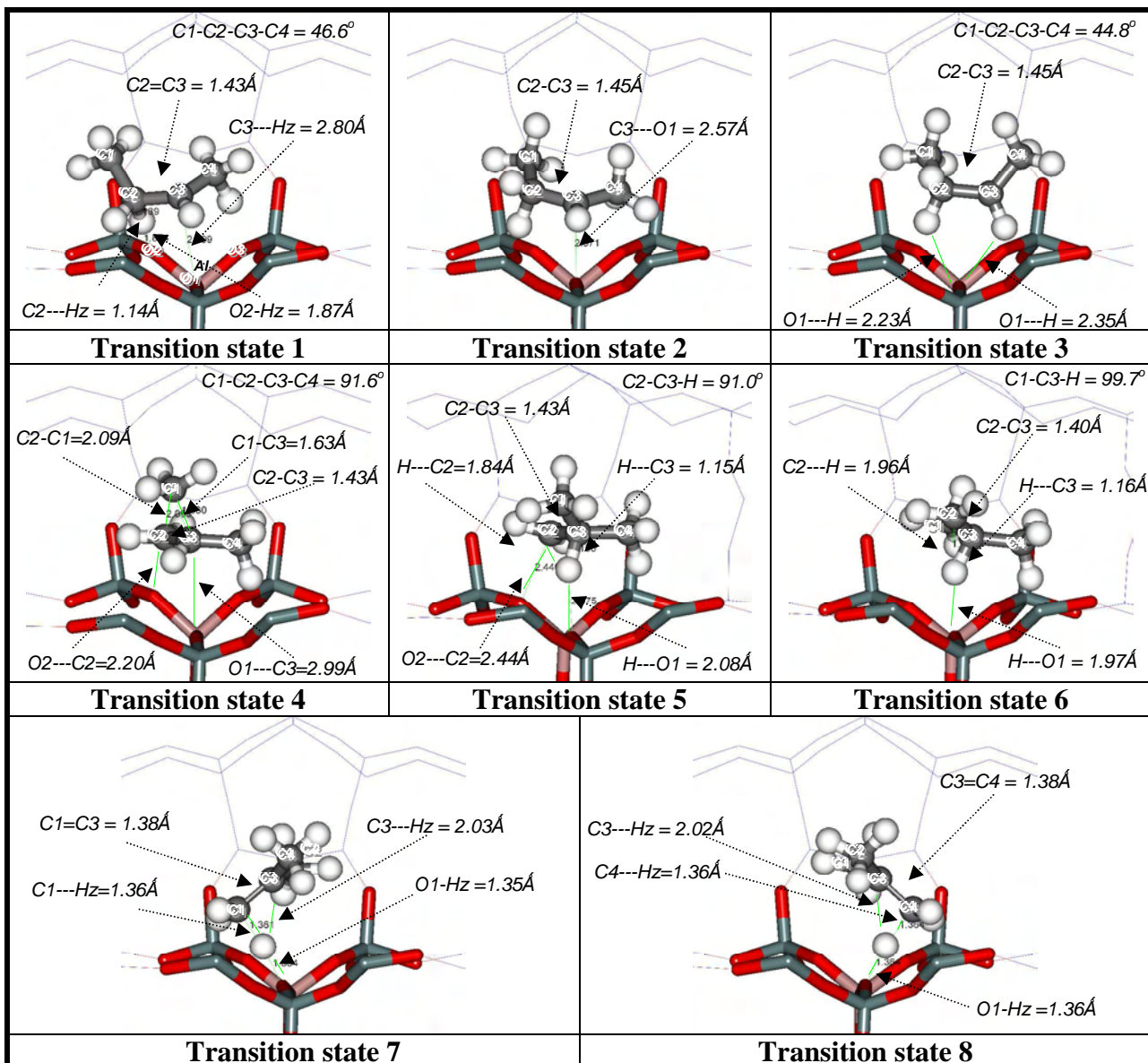


Figure 3 Minima obtained in this study. 6T region denoted using a stick representation and the 21T region using wireframe. Atoms in the foreground have been removed to aid visualisation. Carbon atoms are numbered 1 to 4 to facilitate interpretation. Only the key zeolite atoms are numbered in the top left panel. Key distances and angles are illustrated.



41 Figure 4 Transition states obtained in this study. See Figure 3 caption for additional details.  
42  
43  
44  
45  
46  
47  
48  
49  
50  
51  
52  
53  
54  
55  
56  
57  
58  
59  
60

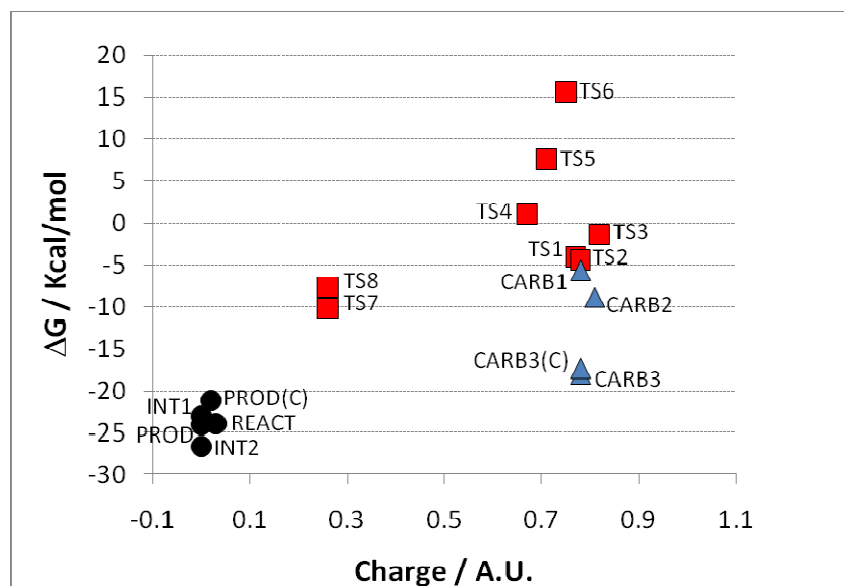


Figure 5 Plot of the zero point corrected single point energies against the Mulliken charge on the alkene. Transition states are denoted by squares (red), carbocations by triangles (blue) and other minima using circles (black).

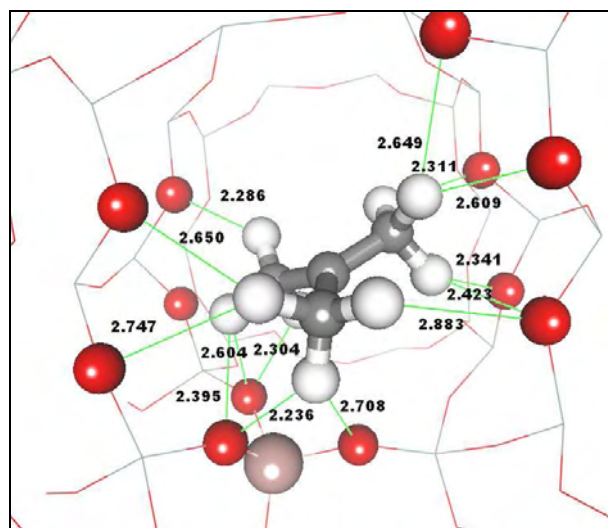


Figure 6 The tertiary butyl carbenium ion obtained in this study (CARB3). The key O---HC interactions are displayed to show the significant stabilizing effect the extended zeolite framework has on this stationary point.

## List of Tables

Table 1 The energies of the stationary points obtained in this study. All energies are relative to the isolated energies of the zeolite model and cis-butene in the gasphase.  $\Delta H$  corresponds to the energy of optimized complexes using the default basis set (M062X with cis-butene and zeolite 6T described by 6-31G(d) and 21T atoms using 3-21G). ZPE corresponds to the zero point correction energy for the optimized stationary points at the default level of theory. DH SP corresponds to the single point energy of the optimized stationary point performed as follows: M062X with cis-butene and zeolite 6T described by 6-311+G(2df,dp) and 21T atoms using 6-31G(d). The  $\Delta G$  (SP+ZPE) value corresponds to the  $\Delta H$  SP plus the ZPE correction obtained using the default basis set calculation. All values are reported in Kcal/mol.

Scheme-A	$\Delta H$	ZPE	$\Delta H$ SP	$\Delta G$ (SP+ZPE)
REACTANT	-22.82	-0.72	-23.25	-23.96
TS1	-4.51	0.44	-4.50	-4.06
CARB1	-6.91	0.42	-6.05	-5.63
TS2	-4.97	0.02	-4.45	-4.43
INT1	-21.65	-3.98	-19.03	-23.01
TS4	-1.31	-1.01	2.08	1.07
INT2	-29.80	-3.18	-23.41	-26.60
TS5	5.39	0.85	6.78	7.63
CARB3	-19.68	0.24	-18.29	-18.04
TS7	-11.38	1.42	-11.62	-10.21
PRODUCT	-20.34	-1.61	-22.50	-24.11

Scheme-B	$\Delta H$	ZPE	$\Delta H$ SP	$\Delta G$ (SP+ZPE)
REACT	-22.82	-0.72	-23.25	-23.96
TS1	-4.51	0.44	-4.50	-4.06
CARB1	-6.91	0.42	-6.05	-5.63
TS3	-1.46	-0.38	-0.94	-1.32
CARB2	-7.96	-0.36	-8.50	-8.87
TS6	13.36	2.11	13.48	15.59
CARB3 (C)	-19.16	0.68	-18.06	-17.38
TS8	-9.72	1.76	-9.38	-7.62
PRODUCT (C)	-18.62	-2.21	-18.94	-21.15

## List of References

(1) Choudary, N.; Newalkar, B. *Journal of Porous Materials* 2010, 1.

(2) Kangas, M.; Kumar, N.; Harlin, E.; Salmi, T.; Murzin, D. Y. *Industrial & Engineering Chemistry Research* 2008, 47, 5402.

(3) Brändle, M.; Sauer, J. *Journal of the American Chemical Society* 1998, 120, 1556.

(4) Macht, J.; Carr, R. T.; Iglesia, E. *Journal of the American Chemical Society* 2009, 131, 6554.

(5) Katada, N.; Suzuki, K.; Noda, T.; Sastre, G.; Niwa, M. *Journal of Physical Chemistry C* 2009, 113, 19208.

(6) Lesthaeghe, D.; Van Speybroeck, V.; Waroquier, M. *Physical Chemistry Chemical Physics* 2009, 11, 5222.

(7) Boekfa, B.; Pantu, P.; Probst, M.; Limtrakul, J. *Journal of Physical Chemistry C* 2010, 114, 15061.

(8) Borgoo, A.; Tozer, D. J.; Geerlings, P.; De Proft, F. *Physical Chemistry Chemical Physics* 2009, 11, 2862.

(9) Boronat, M.; Concepcion, P.; Corma, A.; Navarro, M. T.; Renz, M.; Valencia, S. *Physical Chemistry Chemical Physics* 2009, 11, 2876.

(10) Corma, A. *Chemical Reviews* 1995, 95, 559.

(11) Perego, C.; Ingallina, P. *Catalysis Today* 2002, 73, 3.

(12) Vahteristo, K.; Sahala, K. M.; Laari, A.; Solonen, A.; Haario, H. *Chemical Engineering Science* 2010, 65, 4640.

(13) Maihom, T.; Pantu, P.; Tachakritikul, C.; Probst, M.; Limtrakul, J. *Journal of Physical Chemistry C* 2010, 114, 7850.

(14) Sun, Y. X.; Yang, J.; Zhao, L. F.; Dai, J. X.; Sun, H. *Journal of Physical Chemistry C* 2010, 114, 5975.

(15) de Menorval, B.; Ayrault, P.; Gnepp, N. S.; Guisnet, M. *Journal of Catalysis* 2005, 230, 38.

(16) Asensi, M. A.; Martínez, A. *Applied Catalysis A: General* 1999, 183, 155.

(17) Guisnet, M.; Andy, P.; Gnepp, N. S.; Travers, C.; Benazzi, E. *Journal of the Chemical Society, Chemical Communications* 1995, 1685.

(18) de Ménorval, B.; Ayrault, P.; Gnepp, N. S.; Guisnet, M. *Applied Catalysis A: General* 2006, 304, 1.

(19) van Donk, S.; Bus, E.; Broersma, A.; Bitter, J. H.; de Jong, K. R. *Journal of Catalysis* 2002, 212, 86.

(20) Yoon, J. W.; Lee, J. H.; Chang, J. S.; Choo, D. H.; Lee, S. J.; Jhung, S. H. *Catalysis Communications* 2007, 8, 967.

(21) Rutenbeck, D.; Papp, H.; Ernst, H.; Schwieger, W. *Applied Catalysis A: General* 2001, 208, 153.

(22) Hunger, M. *Microporous and Mesoporous Materials* 2005, 82, 241.

(23) Aerts, A.; Kirschhock, C. E. A.; Martens, J. A. *Chemical Society Reviews* 2010, 39, 4626.

(24) O'Neil Parker Jr, W. *Comments Inorg Chem* 2000, 22.

(25) Fellah, M. F.; Pidko, E. A.; van Santen, R. A.; Onal, I. *The Journal of Physical Chemistry C* 2011, 115, 9668.

(26) Zimmerman, P. M.; Head-Gordon, M.; Bell, A. T. *Journal of Chemical Theory and Computation* 2011, 7, 1695.

(27) Agarwal, V.; Conner, W. C.; Auerbach, S. M. *Journal of Physical Chemistry C* 2011, 115, 188.

(28) Fang, H. J.; Zheng, A. M.; Xu, J.; Li, S. H.; Chu, Y. Y.; Chen, L.; Deng, F. *Journal of Physical Chemistry C* 2011, 115, 7429.

(29) Ananikov, V. P.; Musaev, D. G.; Morokuma, K. *Journal of Molecular Catalysis A: Chemical* 2010, 324, 104.

(30) De Moor, B. A.; Ghysels, A.; Reyniers, M. F.; Van Speybroeck, V.; Waroquier, M.; Marin, G. B. *Journal of Chemical Theory and Computation* 2011, 7, 1090.

(31) Hansen, N.; Kerber, T.; Sauer, J.; Bell, A. T.; Keil, F. J. *Journal of the American Chemical Society* 2010, 132, 11525.

1  
2 (32) Hansen, N.; Brüggemann, T.; Bell, A. T.; Keil, F. J. *The Journal of Physical Chemistry C* 2008,  
3  
4  
5  
6 112, 15402.  
7  
8 (33) Zhao, Y.; Truhlar, D. G. *Theoretical Chemistry Accounts* 2008, 120, 215.  
9  
10 (34) Hohenstein, E. G.; Chill, S. T.; Sherrill, C. D. *Journal of Chemical Theory and Computation*  
11 2008, 4, 1996.  
12  
13 (35) Zhao, Y.; Truhlar, D. G. *Journal of Physical Chemistry C* 2008, 112, 6860.  
14  
15 (36) Boronat, M.; Viruela, P.; Corma, A. *Physical Chemistry Chemical Physics* 2001, 3, 3235.  
16  
17 (37) Gleeson, D. *Journal of Computer-Aided Molecular Design* 2008, 22, 579.  
18  
19 (38) Demuth, T.; Rozanska, X.; Benco, L.; Hafner, J.; van Santen, R. A.; Toulhoat, H. *Journal of  
20 Catalysis* 2003, 214, 68.  
21  
22 (39) Boronat, M.; Viruela, P. M.; Corma, A. *J Am Chem Soc* 2004, 126, 3300.  
23  
24 (40) Boronat, M.; Corma, A. *Applied Catalysis A: General* 2008, 336, 2.  
25  
26 (41) Nieminen, V.; Sierka, M.; Murzin, D. Y.; Sauer, J. *Journal of Catalysis* 2005, 231, 393.  
27  
28 (42) Tuma, C.; Kerber, T.; Sauer, J. *Angew Chem Int Ed Engl* 2010, 49, 4678.  
29  
30 (43) Tuma, C.; Sauer, J. *Angew Chem Int Ed Engl* 2005, 44, 4769.  
31  
32 (44) Rosenbach, N.; dos Santos, A. P. A.; Franco, M.; Mota, C. J. A. *Chemical Physics Letters* 2010,  
33 485, 124.  
34  
35 (45) Svelle, S.; Kolboe, S.; Swang, O. *The Journal of Physical Chemistry B* 2004, 108, 2953.  
36  
37 (46) Mazar, M. N.; Al-Hashimi, S.; Bhan, A.; Cococcioni, M. *Journal of Physical Chemistry C* 2011,  
38 115, 10087.  
39  
40 (47) Material Studio 4.0; Accelrys  
41  
42 (48) Yang, G.; Zhou, L.; Liu, X.; Han, X.; Bao, X. *Chemistry* 2011.  
43  
44 (49) Yumura, T.; Takeuchi, M.; Kobayashi, H.; Kuroda, Y. *Inorganic Chemistry* 2008, 48, 508.  
45  
46 (50) Frisch, M. J.; Trucks, G. W.; Schlegel, H. B.; Scuseria, G. E.; Robb, M. A.; Cheeseman, J. R.;  
47 Montgomery, J., J. A.; Vreven, T.; Kudin, K. N.; Burant, J. C.; Millam, J. M.; Iyengar, S. S.; Tomasi,  
48 J.; Barone, V.; Mennucci, B.; Cossi, M.; Scalmani, G.; Rega, N.; Petersson, G. A.; Nakatsuji, H.;  
49 Hada, M.; Ehara, M.; Toyota, K.; Fukuda, R.; Hasegawa, J.; Ishida, M.; Nakajima, T.; Honda, Y.;  
50 Kitao, O.; Nakai, H.; Klene, M.; Li, X.; Knox, J. E.; Hratchian, H. P.; Cross, J. B.; Bakken, V.;  
51 Adamo, C.; Jaramillo, J.; Gomperts, R.; Stratmann, R. E.; Yazyev, O.; Austin, A. J.; Cammi, R.;  
52 Pomelli, C.; Ochterski, J. W.; Ayala, P. Y.; Morokuma, K.; Voth, G. A.; Salvador, P.; Dannenberg, J.  
53 J.; Zakrzewski, V. G.; Dapprich, S.; Daniels, A. D.; Strain, M. C.; Farkas, O.; Malick, D. K.; Rabuck,  
54 A. D.; Raghavachari, K.; Foresman, J. B.; Ortiz, J. V.; Cui, Q.; Baboul, A. G.; Clifford, S.;  
55 Cioslowski, J.; Stefanov, B. B.; Liu, G.; Liashenko, A.; Piskorz, P.; Komaromi, I.; Martin, R. L.; Fox,  
56 D. J.; Keith, T.; Al-Laham, M. A.; Peng, C. Y.; Nanayakkara, A.; Challacombe, M.; Gill, P. M. W.;  
57 Johnson, B.; Chen, W.; Wong, M. W.; Gonzalez, C.; Pople, J. A. Gaussian 03, Revision C.02;  
58 Gaussian, inc: Wallingford CT, 2004.  
59  
60 (51) Boronat, M.; Zicovich-Wilson, C. M.; Viruela, P.; Corma, A. *The Journal of Physical  
Chemistry B* 2001, 105, 11169.